LOCKHEED ELECTRONICS COMPANY, INC.
AEROSPACE SYSTEMS DIVISION
16811 EL CAMINO REAL • HOUSTON, TEXAS 77058 • TELEPHONE (AREA CODE 713) 488-0080

REF: 641-744
Job Order 75-215
NAS 9-12200

NASA CR-
150 9899

TECHNICAL MEMORANDUM

THE SIGNIFICANCE OF THE S-193 SKYLAB EXPERIMENT USING PRELIMINARY DATA EVALUATION

By

Kumar Krishen

Approved: J. J. Carney

J. J. Carney, Supervisor
EO Exploratory Investigations Section

Distribution:

JSC/L. F. Childs
K. J. Demel
N. M. Hatcher
W. E. Hensley
A. W. Patteson
LEC/O. N. Brandt
D. J. Pounds
W. A. Rosenkranz
R. E. Tokerud
J. O. File
Technical Library (2)
REDAF (3)

Aug. 1974
Issued March 1975

LEC-4250

CONTENTS

TABLES

Figures

S-193 RADIOMETER/SCATTEROMETER/ALTIMETER

1.0 INTRODUCTION

Certain all-weather, night and day, synoptic high resolution ocean observations can best be provided by spaceborne microwave systems. Microwave sensors are attractive for the probing of geological phenomena since penetration through foliage is possible in addition to some surface penetration. The Skylab S-193 Radiometer/Scatterometer/Altimeter experiment was man's first attempt to gather data using earth-oriented, spaceborne, active microwave systems. For the first time nearly simultaneous radiometric brightness temperature and radar backscatter data were acquired over land and ocean scenes using a spaceborne microwave sensor.

The S-193 receiver was designed to measure powers from 10^{-15} watts to 10^{-10} watts, while surviving in an environment with peak transmitted powers of 2,000 watts. This represents an advancement in the microwave remote sensing technology.

The full potential of S-193 program has not been realized since the analysis of the data is continuing. The

experience gained from this program and limited analysis of the data have been used to make noteworthy contributions to the planning of the GEOS-C and SEASAT-A programs. The definition of sensor specifications, mission requirements, data handling, and ground truth coordination for these two NASA programs was directly influenced by the performance of the S-193 sensor.

Recently, NASA organized an Active Microwave Workshop to outline applications and systems for future aerospace programs. The progress in the S-193 data analysis and the results of the aircraft microwave remote sensing programs were reviewed by the workshop participants. As a result of this, the oceans panel recommended design and development of higher precision scatterometer, altimeter, and radiometer for future remote sensing programs.

During the last portion of the Skylab-3 mission, the antenna gimbal malfunctioned. The recommended fix from detailed analysis was to disable the pitch gimbal electrically and pin the antenna in the pitch axis. A procedure was developed, and an astronaut completed the fix in space. The completion of this task has demonstrated that complex electronic systems can be repaired in space, thus extending

their operating life. Techniques for the repair of electronic systems in space can be efficiently employed in the Space Shuttle Program where the electronic systems are expected to operate over extended periods.

S-193 system gathered data in intrack and crosstrack modes over land and ocean surfaces. In addition, data was also gathered looking at deep space, for sensor performance evaluation, and revision to the preflight calibrations. While Skylab-2 was in progress, the first Pacific hurricane of the season named Ava was forming. One objective of S-193 program was to observe hurricanes and regions of high ocean surface wind velocity. With the participation of mission control personnel and the Skylab astronauts, a pass was scheduled over Ava for June 6, 1974. The Skylab-2 problems precluded operating the S-193 sensor in the desired Z-local vertical configuration. However, the flexibility of the sensor modes and data gathered in crosstrack contiguous mode were utilized. A comprehensive remote sensing study of hurricane Ava was accomplished by the joint efforts of NASA and the National Oceanic and Atmospheric Administration (NOAA). These measurements were unusually broad in scope encompassing aircraft, satellite, and Skylab observations

with a number of microwave sensors. This was a first in the remote sensing study of a potential hurricane.

A unique feature of the Skylab S-193 program was the evaluation of the sensor inflight performance. This aspect of the program was highlighted by the deployment and operation of ground-based microwave receivers. The antenna pattern and scan performance, scatterometer transmitted power, pulse rate, and duration were measured by an array of ground-based receivers. The primary purpose of this study by the University of Kansas was to measure changes in antenna performance which might have resulted from the launch and the space environments. For the evaluation of the altimeter transmitter and receiver performance the NASA Wallops Space Center receiver station was employed. The altimeter pulse shape, duration, spacing, and amplitude were recorded. In addition, data was gathered over targets with known physical, electrical, and scattering characteristics, such as smooth water surfaces, deep space, Great Salt Lake Desert, and White Sands, N. M. The results of the S-193 sensor performance evaluation have been used in revising the data processing to reflect the actual inflight performance of the sensor. More important, a methodology has been developed for the inflight evaluation of future spaceborne microwave sensors.

The progress made in the development of microwave technology toward more sophisticated future spaceborne earth-oriented microwave sensors, the investigations of earth phenomena, and the procedures for future missions resulting from the S-193 program should be taken with caution. This progress should only represent a significant step toward the ultimate goal of using operationally the spaceborne microwave sensors for sensing earth resources phenomena. Future microwave programs demand development of high precision side-looking imaging radars, in addition to scatterometers, altimeters, and radiometers. Multiple frequency, multiple polarization, and better antenna design features are envisaged for future sensors.

2.0 SUMMARY OF S-193 OPERATIONAL MODES

2.1 RADIOMETER/SCATTEROMETER

The radiometer and scatterometer can operate in various scanning and polarization modes jointly and separately[1]. A summary of these modes is given in table 1 and briefly explained in the following sections.

2.1.1 Intrack Noncontiguous (ITNC) Mode

This mode is used for a joint radiometer and scatterometer operation. In this mode, only the pitch angle is varied. A resolution cell on the ground (figure 1) is seen by the radiometer and scatterometer at approximately the following pitch angles: 0 degrees, 15.6 degrees, 29.4 degrees, 40.1 degrees, and 48 degrees.

In the sequence mode (polarization switch position 5) during each dwell at a given pitch angle, all the following measurements are taken:

- Scatterometer data with VV, HH, VH, and HV polarizations
- Radiometer and noise data with V and H polarizations
- Radiometer reference voltages R_1 and R_2

TABLE I. — NOMINAL RADIOMETER/SCATTEROMETER MODES

Operation	Scanning mode choice	Polarization choice	Pitch angles
Radiometer/scatterometer	1. Intrack Noncontiguous mode (ITNC)	1. Scatterometer VV, HH, VH, and HV Radiometer V and H	0, 15.6, 29.4, 40.1, and 48 degrees
		2. One polarization combination (VV or HH or HV or VH) for scatterometer, and V or H for radiometer	
Radiometer/scatterometer	1. Cross track Contiguous (CTNC) left/right	Same as for ITNC	Same as for ITNC
	2. CTNC, left		
	3. CTNC, right		
Radiometer/scatterometer	1. Intrack Contiguous (ITC) mode	1. One polarization combination for scatterometer (VV or HH or VH or HV) for scatterometer and V or H for radiometer	Same as for ITNC
Radiometer/scatterometer	1. Cross track contiguous (CTC) left/right	1. VV or HH for scatterometer and V or H for radiometer	+11° to -11°
Scatterometer only	1. CTC	1. V and H radiometer data	+11° to -11°
Scatterometer only	1. CTC	1. Scatterometer data for VV and HH	+11° to -11°

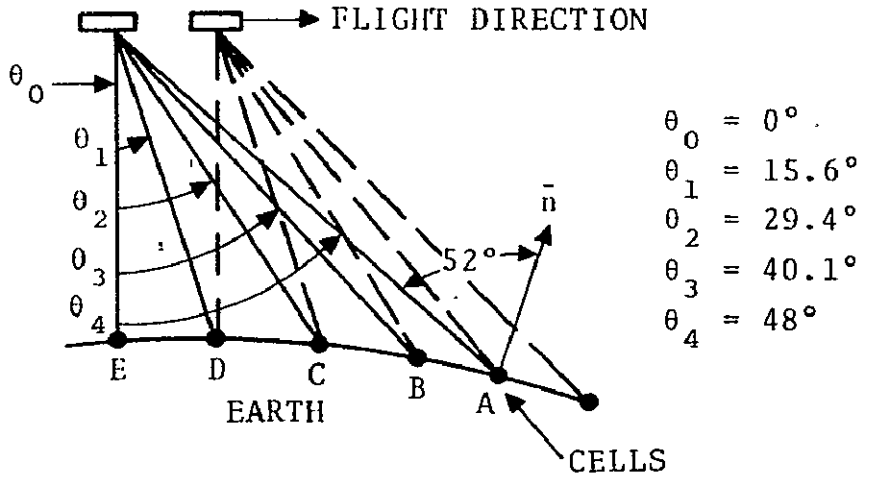

Figure 1 . — Intrack noncontiguous scan mode (ITNC).

There is a choice of other polarization settings: VV (switch position 1), VH (switch position 2), HV (switch position 3), and HH (switch position 4) for this mode.

The complete scan cycle time in this mode is 15.25 seconds. The roll angle is always zero.

In reviewing the S-193 radiometer/scatterometer Skylab-acquired data, it was determined that some scan angle positions in this mode were different from the nominal prelaunch values. The angles, 0 degrees, 15.6 degrees, and 29.4 degrees, are not markedly different. However, the 40.1-degree and 48-degree angles show noteworthy change. In particular, the last angle (the nominal value before launch was 48 degrees) remains, for most part, within 46 to 47 degrees. The 40.1-degree angle is for most data within 1.5 degrees of the design specification.

During Skylab-3, the antenna gimbals malfunctioned. The ITNC mode has not been in operation after this happened. No data has been gathered in this mode during the Skylab-4 mission.

2.1.2 Crosstrack Noncontiguous (CTNC) Mode

In this mode, the roll angle is varied identically to the intrack noncontiguous mode, and the pitch angle remains zero. The motion of the field of view (FOV) is shown in figure 2, where it can be seen that individual cells are viewed from only one antenna position. Because of the motion of the antenna in the pitch direction, the cells lie on a curved arc. There are three forms of this mode, left scan, right scan, and left/right scan as shown in the figure. The outermost cell is viewed at approximately 52 degrees (corresponding to 48-degree gimbal angle) and the innermost cell at approximately 0 degrees at all times.

The total scan time for a complete cycle is 15.25 seconds. Only combined radiometer/scatterometer data can be gathered in the CTNC mode. In the sequence mode (polarization switch setting 5), data for all polarization combinations is gathered automatically for radiometer and scatterometer systems.

The polarization setting can be changed to gather data for VV (switch position 1), VH (switch position 2), HV (switch position 3), and HH (switch position 4) individually.

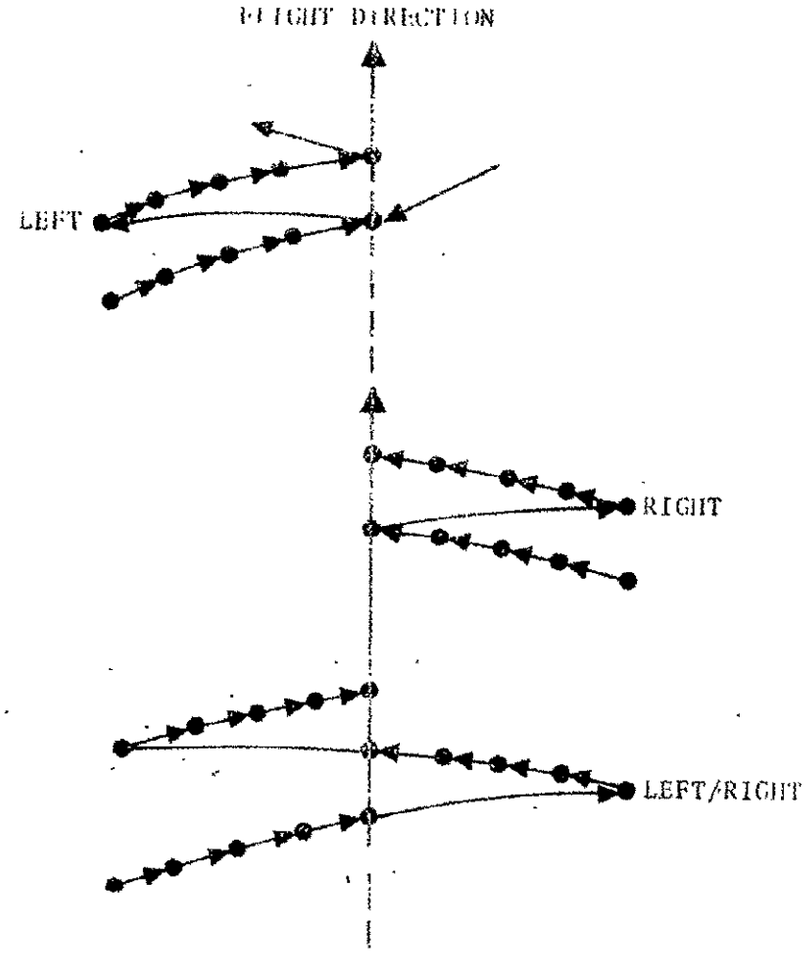

Figure 2 . — Cross-track, noncontiguous mode.

The S-193 data for the CTNC mode shows that the antenna scan angles are approximately the same for 0-degree, 15.6-degree, and 29.4-degree angles. The 40.1-degree pitch angle reaches only 37.5 degrees for the Skylab-acquired data. The right scan extends up to approximately 43 degrees instead of the nominal prelaunch value of 48 degrees, and the left scan extends up to 46 degrees instead of 48 degrees. Some oscillation in the antenna pitch angle is also noticeable at each dwell angle. Skylab-4 mission antenna scan motion was also variable.

2.1.3 Intrack Contiguous (ITC) Mode

The pattern is similar to the intrack noncontiguous mode (figure 3), except that the antenna is scanned much faster and there is no dwell at any antenna pitch angle. The entire inflight path is eventually scanned at all incidence angles with this process.

The scan cycle time is chosen so that at the vehicle velocity the resolution cell at incidence angle 48 degrees overlaps the previous cell by approximately 25 percent, the 40.1-degree cell overlaps its predecessor by less than 20 percent, etc., down to the 0-degree incidence angle

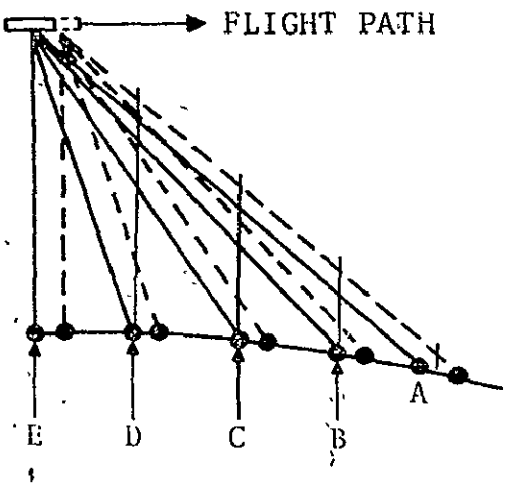

Figure 3 . – Intrack contiguous mode.

case where gapping rather than overlap occurs. The complete cycle for one scan takes about 4.0 seconds.

The radiometer data is taken during slew periods between two pitch angles corresponding to scatterometer data angles. In this mode during a given pass, only one transmitted polarization can be chosen. Data corresponding to the vertical or horizontal polarization is received in addition to data similar to the received polarization for the radiometer. As the vehicle progresses on successive scans, the entire path is viewed at 48 degrees and less, except for gapping at lowest angles.

In the ITC mode, the starting angle was about 43 degrees (it should have been 48 degrees) during the Skylab-2 and 3 missions. Since the Doppler filters are centered around 48 degrees, the scatterometer data recorded for 43 degrees is highly attenuated. Corrections for the Doppler filter attenuation have been implemented into the NASA/Computations and Analysis Division S-193 processing program. Other angles are also slightly off. The difference increases with increasing pitch angle. However, no correction to the scatterometer data is needed at the angles other than the highest angle (43 degrees).

During the Skylab-3 mission, a malfunction occurred in the antenna gimbals. The pitch gimbal has been disabled as a fix. Consequently, no data has been gathered in the ITC mode after the malfunction.

2.1.4 Crosstrack Contiguous (CTC) Mode

This mode contains three submodes:

- Radiometer/scatterometer (RAD/SCAT) — In this submode, the astronaut can select one inphase polarization pair, vertical transmit/vertical receive (VV), or horizontal transmit/horizontal receive (HH).
- Radiometer (RAD) — In this submode, data corresponding to vertical and horizontal polarization will be gathered.
- Scatterometer (SCAT) — In this submode, data for VV and HH polarization combinations will be gathered.

This mode provides a side-to-side linear scan covering ±11.375 degrees and a turnaround to repeat. As can be seen in figure 4, this is a mapping mode. To compensate for the satellite forward velocity which could cause skewing of the pattern perpendicular to the flightpath, the pitch gimbal is scanned backwards slightly as the roll angle oscillates between its limits. Measurements are made for every 1.896 degrees of beam center motion, ranging from -11.375 degrees to +11.375 degrees in roll. The total time of one cycle is 4.24 seconds. The pitch offset angles for this mode can be chosen as incidence angles of 0 degrees, 15.6 degrees, 29.4 degrees, or 40.1 degrees.

A study of Skylab-acquired data in the CTC mode revealed that the scan extends only up to a total of about 20.6 degrees instead of 22.75 degrees. The repeatability of the timing sequence also differs from that indicated by this figure.

Because of antenna malfunction during the Skylab-3 mission, the pitch gimbal was fixed. Consequently, the scans on the ground are not parallel for the Skylab-4 (SL-4) mission. The roll angles are also different in SL-4 data.

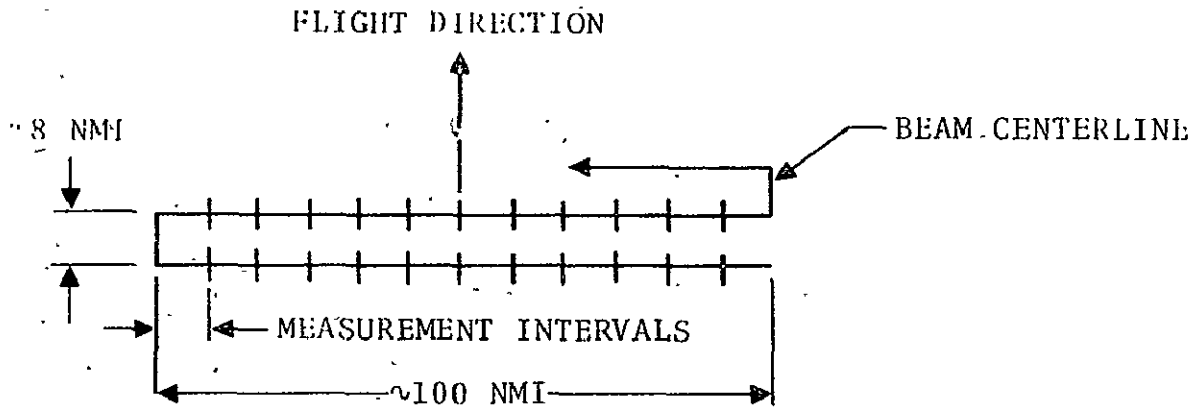

Figure 4 . — Cross-track contiguous mode.

2.2 ALTIMETER

The altimeter may also be operated in several modes (table 2). Within each mode the altimeter is automatically sequenced through several submodes to provide internal calibrations and engineering information for use in the design of future short-pulse radar systems operating at Earth satellite altitudes. The pulse repetition frequency is 250 pulses per second in all modes. Briefly, the purpose and operation of each mode is as follows[1].

2.2.1 Mode I - Pulse Shape

The purpose of this mode is to measure the return pulse shape with the antenna pointing at nadir and off nadir. Individual return pulses are square-law sampled and recorded for different sets of system parameters. In this mode the pulse width is 100 ns. Sample-and-hold gate spacing is 25 ns, and IF filter bandwidth is 10 MHz and 100 MHz. The antenna is pointed at nadir and at a pitch angle of 0.43 degrees off nadir. The total running time of the data acquisition submodes (DAS's) is 179 s.

TABLE 2. – NOMINAL S-193 ALTIMETER MODES

Mode	Antenna pointing angles	Pulse width	Sample and hold gate spacing	Total data acquisition time
I. Pulse shape	Nadir 0.43° off nadir	100 ns	25 ns	179 s
II. Backscatter Cross Section	0.4°, 1.3°, 2.65°, 7.56°, and 15.6	100 ns	25 ns	174 s
III. Time correlation	Nadir	10 ns 100 ns	25 ns 10 ns	147.7 s
IV. Frequency Correlation	Deleted →			
V. Pulse	Nadir	100 ns 10 ns 130 ns	25 ns 10 ns	174.7 s
VI. Nadir Alignment	off nadir to nadir	100 ns	NA	200 s

2.2.2 Mode II - Cross Section

The purpose of this mode is to measure the radar backscatter coefficient (σ_o) with the antenna pointing at nadir and off nadir. The off-nadir antenna angles are 0.4, 1.3, 2.65, 7.56, and 15.6 degrees. Pulse width is 100 ns, and IF filter bandwidth is 10 MHz. Sample-and-hold gate spacing is 25 ns. The AGC voltage is the primary recorded function in this mode because σ_o is determined from this voltage measurement. A two-point calibration of the AGC loop is included in this mode to provide a correction to the calculated σ_o. The total running time for the DAS's is 174 s.

2.2.3 Mode III - Time Correlation

The purpose of this mode is to measure the range-gated correlation between pairs of pulses with variable time spacing. The pulses are transmitted at a rate of 250 pulse pairs per second. Individual return pairs are square-law sampled and recorded for different sets of system parameters. The antenna is pointed toward nadir throughout this mode. Pulse width is 10 and 100 ns, and IF filter bandwidth is 100 MHz and 10 MHz. Sample-and-hold gate spacing is 25 and 10 ns. The total running time for the DAS's is 147.7 s.

2.2.4 Mode IV - Frequency Correlation

This mode was deleted during the development of the altimeter.

2.2.5 Mode V - Pulse Compression

The purpose of this mode is to make measurements for use in comparing the ocean return signal characteristics for a 100-ns and a 10-ns uncoded pulse with the return signal characteristics for a coded 130-ns transmitted pulse compressed to 10 ns within the receiver. Sample-and-hold gate spacing is 25 ns for the 100-ns pulse and 10 ns for the 10-ns and 130-ns pulses. The total running time for this mode is 174.7 s.

2.2.6 Mode VI - Nadir Align

The purpose of this mode is to accomplish nadir alignment of the S-193 antenna. Alignment with the subsatellite point is automatically sought in this mode. It is implemented by using the AGC control voltage from the altimeter. The antenna is automatically moved in pitch and roll to the position where AGC control voltage is a maximum. This antenna position is then redesignated as the nadir position.

The transmitted pulse width is 100 ns, and IF filter bandwidth is 10 MHz. There are no sample-and-hold gates in this mode. The running time for nadir alignment is typically 200 s.

3.0 EXPERIMENT OBJECTIVES AND RESULTS

The analysis of S-193 data is presently continuing. The data is being processed using more accurate calibrations determined from the analysis of S-193 acquired data. Limited analysis of the Skylab S-193 data has demonstrated partial fulfilment of the experiment objectives. A brief summary of the potential experiment objectives and corresponding results will be presented. The experimental results are given following each objective.

3.1 DATA AND RESULTS FOR FUTURE SENSOR DESIGN

One fundamental rationale for the design of the S-193 was to gather data to be used for the design of future satellite radar (altimeter, scatterometer, and side-looking radar) and radiometer systems. Toward this, several scanning, polarization, and pulse modes were incorporated in the S-193 design. Specific results from the data analysis are given in the following section.

3.1.1 Recommendation for Future Radiometer/Altimeter /Scatterometer Design

Recommendations for future radiometer/altimeter scatterometer design based on S-193 data analysis to date are as follows:

Angles of incidence	
Radiometer	0 to 50 degrees
Scatterometer	0 to 50 degrees
Dynamic range	
Radiometer	0 to 350 degrees Kelvin (K)
Scatterometer	50 decibels (dB)
Altimeter	45 dB
Precision	
Radiometer	±1 degrees K minimum ±0.4 degrees K desired
Scatterometer	±0.5 dB minimum ±0.2 dB desired
Altimeter	±10 centimeters
Accuracy	
Radiometer	±1.0 degrees minimum ±0.5 degrees desired (Actual performance at low performance at low temperatures is acceptable.)
Scatterometer	±0.2 dB desired ±0.5 dB minimum
Altimeter	±10 centimeters

Signal-to-noise (S/N) ratio

Scatterometer	25 dB minimum
Altimeters	25 dB minimum

Polarization isolation

Radiometer	20 dB minimum
Scatterometer	25 dB minimum (HH and VV only) 40 dB desired (VH and HV)

Antenna footprint resolution

Radiometer/ scatterometer	Over water	4 miles or less
	Over land	3 miles or less
Altimeter		2 miles or less

Antenna scan performance

Over water	CTNC ITNC and a conical scan
Over land	CTC (pitch offsets 0 degrees, 15 degrees, 30 degrees) ITC

Polarization

Radiometer	V and H
Scatterometer	VV, HH, VH, and HV

3.1.2 Data Handling and Processing

Experience with S-193 indicates that it is of primary importance to begin consideration of data handling at the time of the specification and instrument design.

Close cooperation between design engineers, scientists, and computer programmers throughout the design, development, construction, and testing of the instrument will minimize problems encountered after scientific data collection begins. The data processing algorithms should be developed before system testing begins and used in conjunction with raw system test data to finalize the algorithm and evaluate the systems performance.

The nature of microwave sensors, particularly passive sensors; is such that multipass (generally two-pass) data processing is necessary to obtain best results; since noise sources are required to calibrate radiometers, the calibration and baseline data is by its very nature noisy. To provide the test calibration, the noisy calibration data should be integrated for 5 to 25 times the length of the measurement time. To provide single calibration times this long would be wasteful of observation time; therefore, a number of short calibrations centered about the observation time should be averaged together in some manner. This could be done either by a "look ahead" capability in the data processing system which requires keeping large volumes of data in core storage or, more efficiently, by using a two-pass data processing system. After early efforts to maintain

single-pass processing of S-193 radiometer data produced marginal to unsatisfactory results, a quasi, two-pass system has evolved[2].

3.1.3 Antenna Gimbals and Pointing

Two antenna gimbal failures were recorded – one in pitch during SL-3 and one in roll during SL-4. These failures imply that a more reliable antenna scanning mechanism should be designed for an operational sensor. At the beginning of the Skylab-mission the astronauts installed a device on S-193 designed by General Electric to restore as much of S-193's scanning capability as possible. Operation of the roll gimbal was restored, but the operation of the pitch gimbal was disabled. This allowed normal operation of the crosstrack modes to be restored and permitted nearly normal operation.

The accuracy of a number of experiments including the Antenna Pattern Experiment by the University of Kansas was limited by the pointing accuracy of S-193[3]. At least two factors were involved.

- The attitude of Skylab was not known to have sufficient accuracy to pinpoint the center of the antenna field-of-view on the ground.

- The angular readouts of roll and pitch were not adequate for determining field-of-view to the required accuracy.

In future microwave programs, more attention should be given to the determination of accurate pointing for radiometer and scatterometer systems.

3.1.4 Radiometer Integration Times

The four different integration times used by the radiometer had different effective gains. This made averaging the calibrations and baselines taken at the different angles in noncontiguous modes difficult. The fact that the data processing had no "look ahead" capability combined with the instrument's data taking before the accompanying calibration and baseline data make data processing in the noncontiguous modes difficult. Some error is undoubtedly introduced by the attempt to normalize and average the calibrations and baselines taken at different antenna angles and through different integrators. However, this error appears to be significantly less than the noise that would be introduced by using only the single appropriate calibration.

Consequently, a single radiometer integration time is recommended for future systems. Otherwise each integration time must be thoroughly characterized.

3.1.5 Radiometer/Scatterometer Math Models

During S-193 sensor performance evaluation efforts a method of modeling the S-193 radiometer and scatterometer electronics hardware was developed by Lockheed Electronics Company personnel for NASA/Johnson Space Center[4]. This model has been programmed on a time-showing computer system and was used to improve the S-193 radiometer data reduction equations. This modeling technique can be easily applied to existing noncoherent microwave systems for improved accuracy in data reduction and to proposed systems for optimizing specification, design, and predicting sensor performance.

3.1.6 Polarization Isolation

To meet the constraints of a shroud envelope, the focal length to diameter ratio of the S-193 antenna was reduced. This factor, plus limitations in the antenna feed and microwave switching network, resulted in low isolation between the vertical and horizontal antenna polarization ports. Based on present estimates of cross coupling from the University of Kansas, the ratio of power received in desired polarization to power received in the undesired polarization for the radiometer was only approximately 10 to 13 dB.

An attempt to make a first order correction for this mixing of energy from two polarizations is performed in production data processing. Exact correction is more difficult.

For the scatterometer the condition is more complex. Small errors are generated in the vertical transmit vertical receive (VV) and horizontal transmit horizontal receive (HH) modes. However, in the cross polarized modes, vertical transmit horizontal receive (VH) and horizontal transmit vertical receive (HV), the situation is extremely difficult.

Crossed polarized return signals are generally 10 to 15 dB below the level of like polarized return signals. Since the antenna provided only about 20 dB of isolation on transmission or reception between polarizations, extraneous-like polarized return signals only 5 to 10 dB below the power of the desired cross polarized signals are introduced into the data. An undesired signal (5 dB lower in power) added to a desired signal of the same frequency can cause errors as large as +1.9 to -3.5 decibels depending upon the phase relationships between the two. The stochastic nature of the return signals may contribute to increasing this error. Consequently, a large uncertainty must be assigned to the cross polarized scatterometer data.

3.1.7 Antenna Feed Design

Photographic evidence indicated that the antenna cap was present during SL-4 rendezvous but absent during SL-4 undocking. Data analysis indicates that the cap was absent during all SL-4 data taken.

It should be noted that the quartz on which the cap was mounted had two built-in necks which would have weakened it structurally. It may have been cracked by stresses induced during the launch or gimbal failure during SL-3.

Therefore, it appears that a strong mechanical design in the feed structure is indicated for future sensors.

3.1.8 Results from Comparison of S-193 and S-194

Passive microwave systems on one frequency can be successfully operated in the vicinity of active microwave systems provided careful attention is paid to the design and placement of each.

A radiation cooled reference load for radiometers can be used in space instead of a hot load to improve instrument calibration.

3.1.9 Ground Reflectivity Models

Data for a catalog of backscatter and radiometric brighteness temperatures was acquired by S-193. Construction of a catalog is now in progress at the University of Kansas. From this catalog, ground reflectivity models to be used for the design of future earth-oriented, side-looking radar systems can be developed.

3.1.10 Altimeter Design Results

From the pulse-to-pulse correlation experiments the feasibility of determining the direction of the nadir offset angle was established. The 250 pulses per second were found to give essentially uncorrelated return pulses.

The altimeter pulse compression mode employed a 13-bit Barker code technique to compress a coded 130-ns transmit pulse to 10-ns within the receiver. This mode did not function properly on Skylab-2 and 3 missions. In spite of problems, the Skylab-4 data analysis shows an 8 to 9-dB increase in the signal-to-noise ratio due to the pulse compression[5].

Sufficient data has been gathered to provide pulse width, power, and bandwidth parameters for future design. Data analysis is continuing at this time.

The nadir align mode performed as was expected from the design. It provided alignment to ±0.5 degrees. With the help of this mode more accurate range setting was possible.

3.2 COMBINED RADIOMETER AND SCATTEROMETER OPERATION

This operation will explore the advantage offered by measuring nearly simultaneously the radiometric brightness temperature and radar backscatter over Earth's surface in providing added remote sensing capability as opposed to using only one type of system. In addition, utilizing radiometer to correct scatterometer-acquired backscatter data for atmospheric effects will be studied.

One example of the complementary role of the active and passive measurements is afforded by examining the response of S-193 scatterometer and radiometer to hurricane Ava shown in figures 5 and 6[6,7]. This data is for the highest pitch angle averaging 46.6 degrees in the Cross Track Noncontiguous Radiometer/Scatterometer mode. The approximate areas for the scatterometer data are shown in figure 7. The hurricane Ava composite photograph was prepared by NOAA. During this pass, Skylab was in solar inertial mode. The scatterometer backscattering cross section drop after GMT 18:58:17 (figure 5) is due to the attenuation by the system 0-degree Doppler filter. The dashed line, marked 1 dB bandwidth point, corresponds to a Doppler filter attenuation of 1 dB.

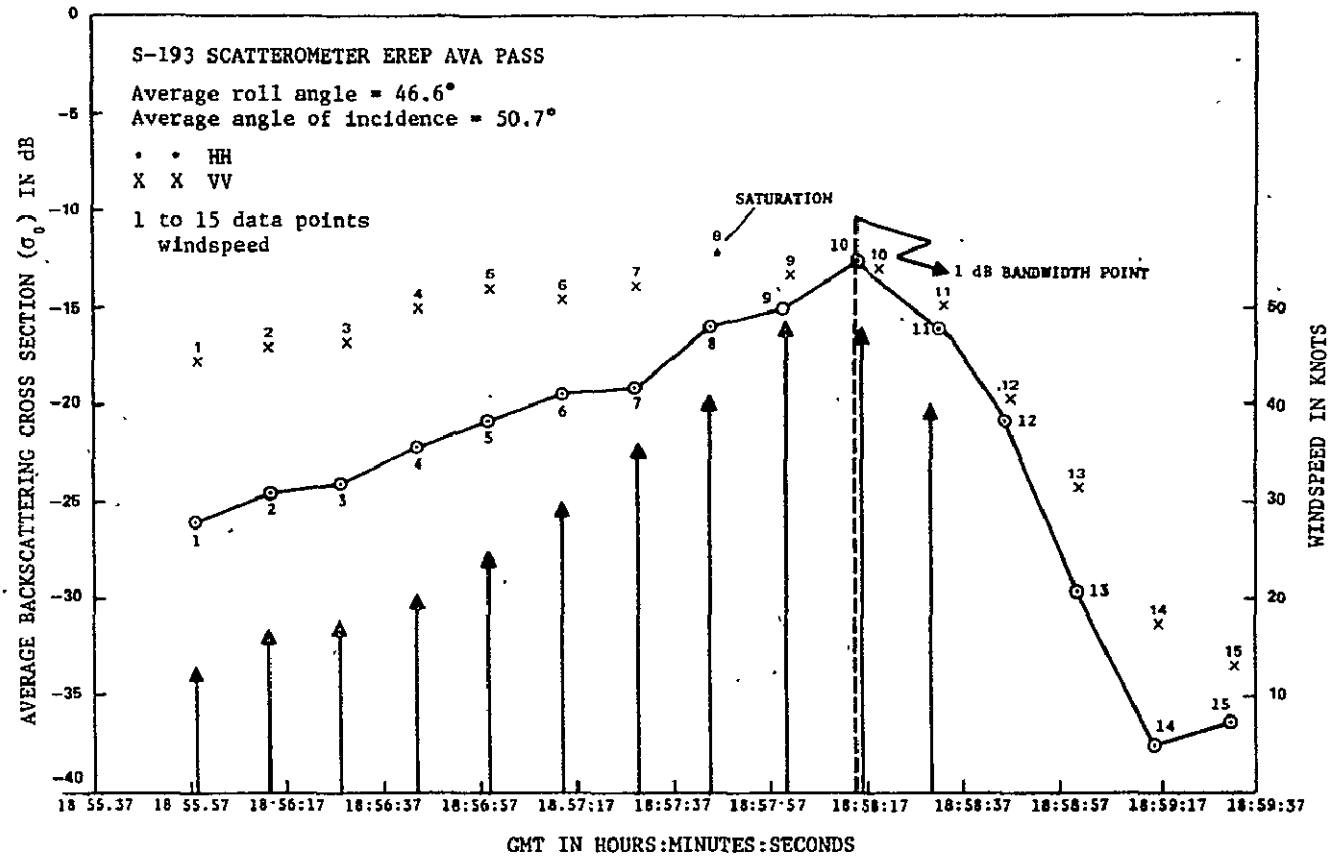

Fig. 5. — Backscattering cross section as a function of time for Hurricane Ava pass with 46.6° roll angle.

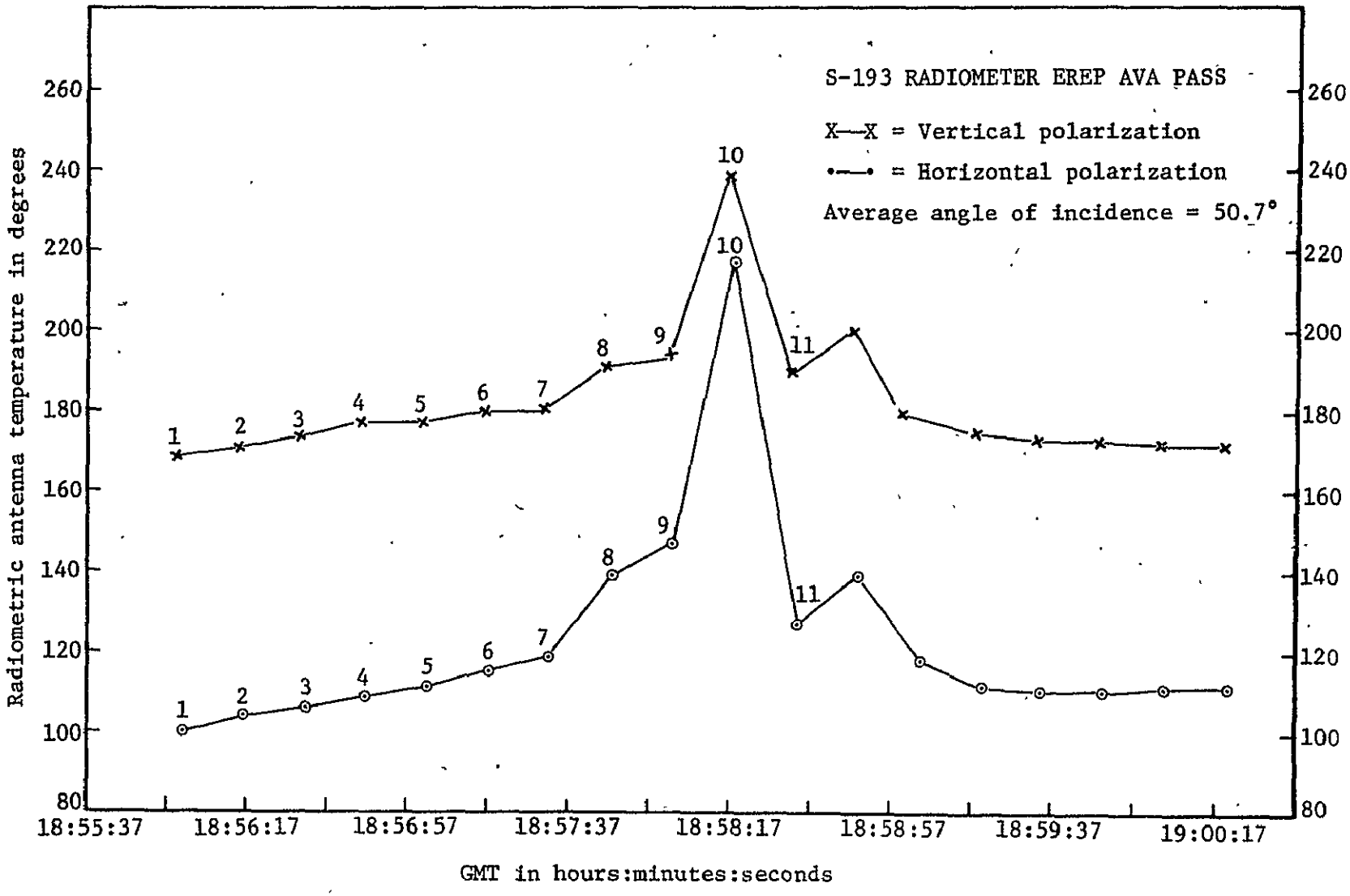

Fig. 6. — Radiometric antenna temperatures for Hurricane Ava pass.

HURRICANE AVA, JUNE 6, 1973, NOAA 2 COMPOSITE

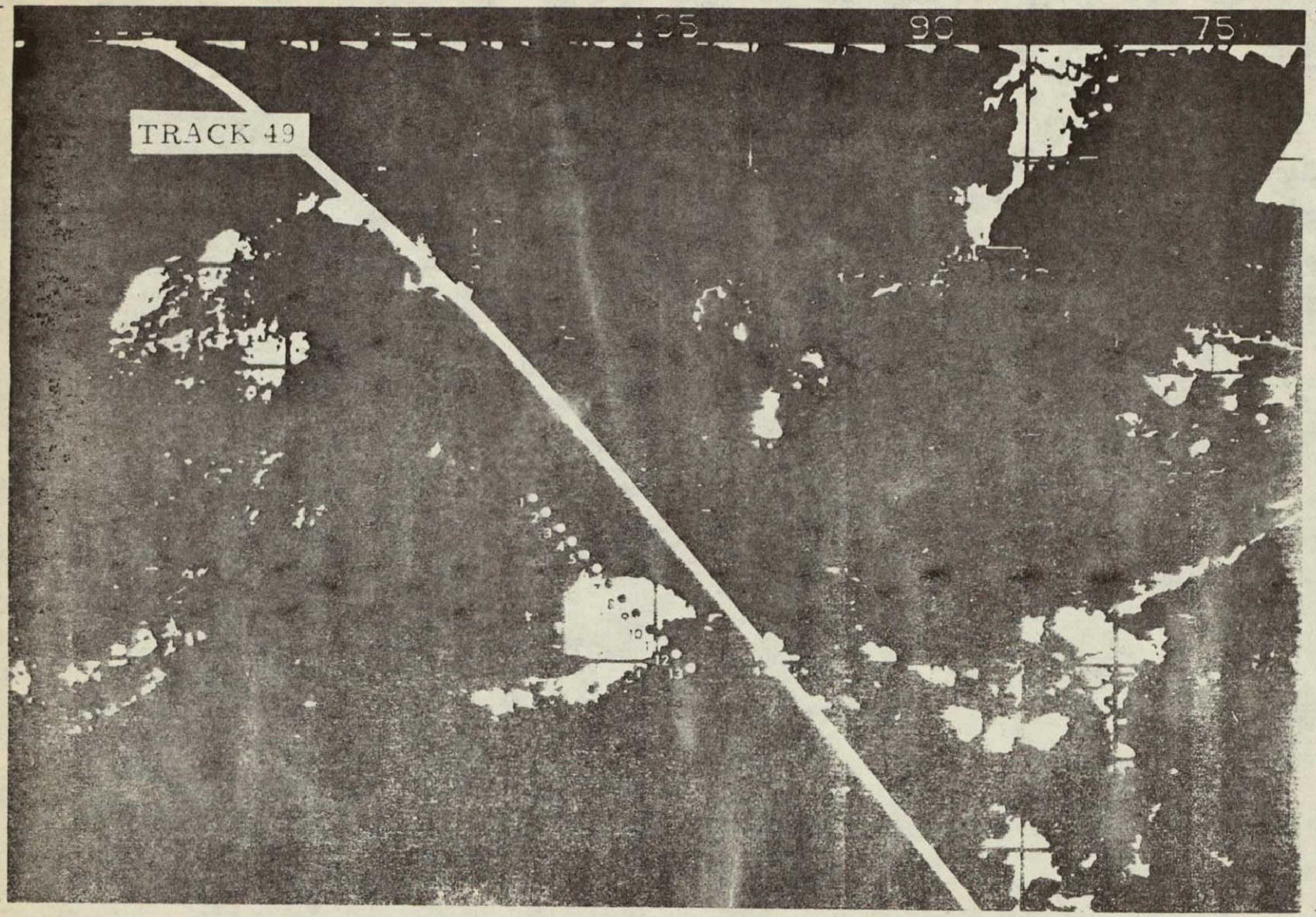

Fig. 7. – Approximate location of the 13 data points (1 through 13) from north to south.

Figure 6 shows that the radiometric antenna temperatures do not increase significantly for surface windspeeds up to about 30 knots. For this range of windspeeds the backscattering cross section (horizontal-transmit, horizontal-receive) increases significantly (figure 5). For 30 to 50 knots the scatterometer backscattering cross section shows markedly decreased dependence; on the other hand, the radiometric antenna temperature rises significantly. Summarizing, the scatterometer-measured backscatter depends strongly on ocean windspeeds up to 30 knots. For higher windspeeds the radiometric antenna temperatures show markedly increased sensitivity to the winds compared to the scatterometer. The increase in the radiometric antenna temperature for higher windspeeds is due to foam. Thus, a larger range of ocean surface winds can be monitored by a combination of radiometer and scatterometer as compared with a single system. In addition, scatterometers can be used to detect surface wind direction while the radiometers do not appear to show this dependence.

A crosstrack contiguous radiometer/scatterometer mode was exercised during EREP pass 5 over Great Salt Lake Desert (figure 8). The scatterometer data for the two scans in figure 8 is shown in figure 9. The dashed curve in figure 9

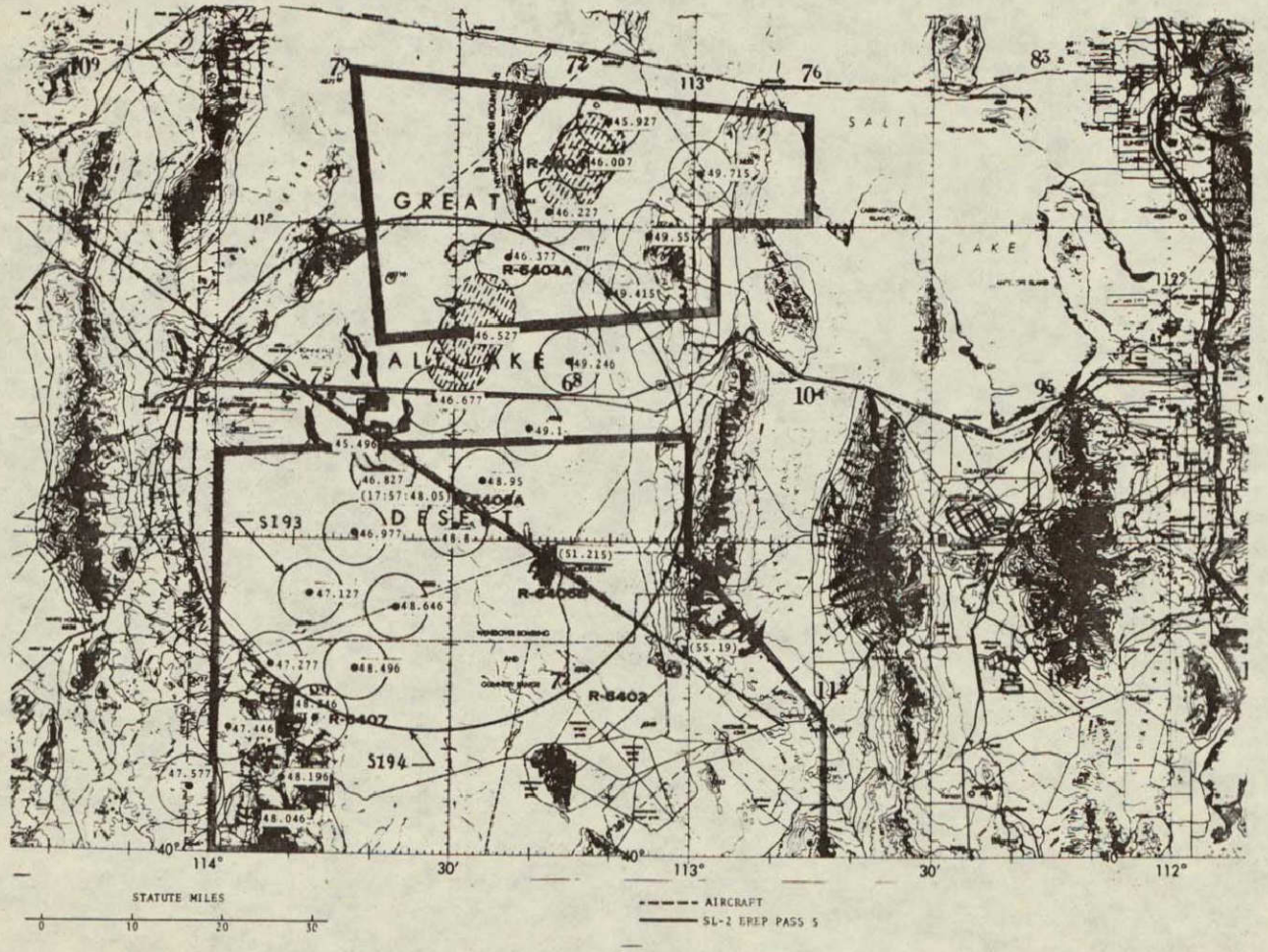

Fig. 8. – Field of view and ground track for Great Salt Lake Desert.

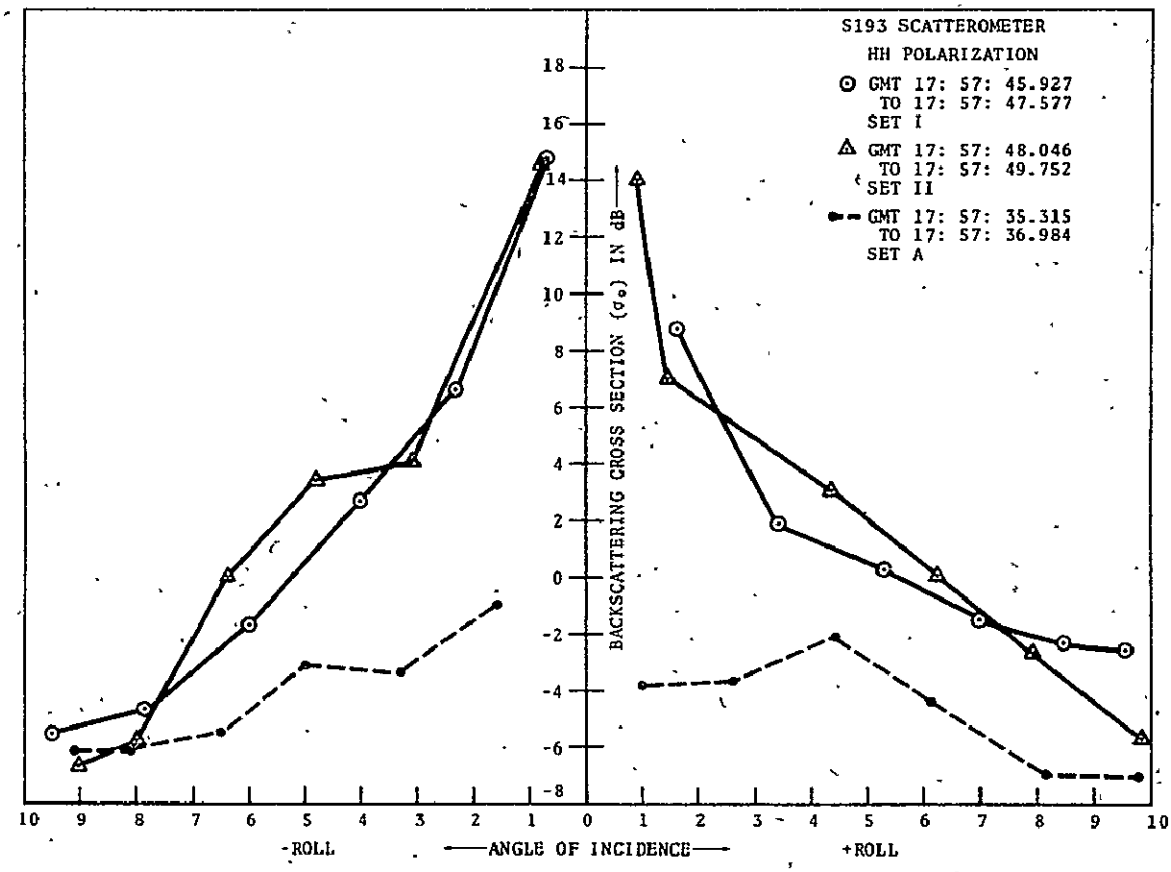

Figure 9. – Comparison of backscattering cross sections, Great Salt Lake Desert and vicinity.

is for an area about 50 miles earlier and is given for comparison purposes. The dashed area (figure 8) shows the extent of the illuminated area for a typical scatterometer measurement in this mode. The radiometer data taken between scatterometer is shown in figure 10.

Comparison of dashed and solid curves in figure 9 shows the specular scattering for the two scans. The scatterometer data can be used to predict the root mean square slope for this area[8]. However, since the area is smooth, the presence of a variation in moisture is difficult to deduce from the scatterometer data. Interpretation of the radiometer data makes it possible to conclude that low radiometric antenna temperatures (of about 200 degrees) are caused by moisture in salt areas. The same phenomena was observed by aircraft and S-194 radiometers. Here again, the complementary role of radiometer and scatterometer is helpful in the interpretation of a physical phenomena.

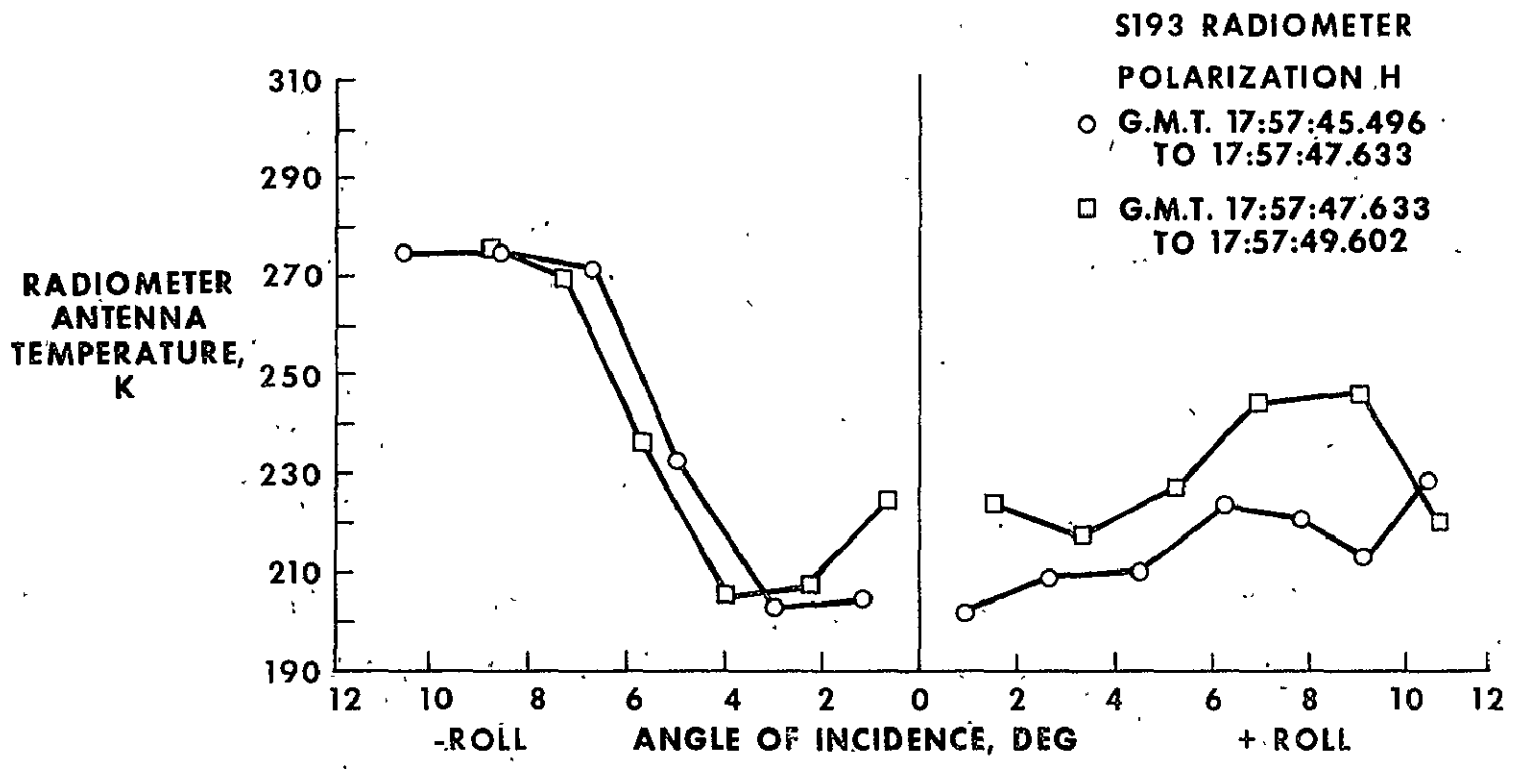

Figure 10. — Radiometer antenna temperature as a function of angle of incidence, Great Salt Lake Desert.

3.3 APPLICATIONS OF MICROWAVE SENSORS TO REMOTELY SENSING EARTH RESOURCES PHENOMENA

3.3.1 Radiometer/Scatterometer

3.3.1.1 Measurement of ocean surface wind/wave fields. One potential objective of S-193 radiometer/scatterometer systems was to determine feasibility of measuring global patterns of ocean surface wave conditions and surface wind fields.

Analysis of S-193 radiometer/scatterometer data to date shows a strong dependence of the backscatter and radiometric brightness temperature on the ocean surface windspeed [9,10, 11,12,13]. Hurricane Ava provided a wide range of surface winds. The preliminary wind field derived from aircraft and reported surface measurements is shown in figure 11[9,14]. For the 46.6-degrees roll angle, the scatterometer backscatter measurements were taken over areas ranging in surface windspeed from 10 to approximately 48 knots (figure 5). The backscatter for HH polarization (σ_{OHH}) increases as the eye of the hurricane is approached. To study the

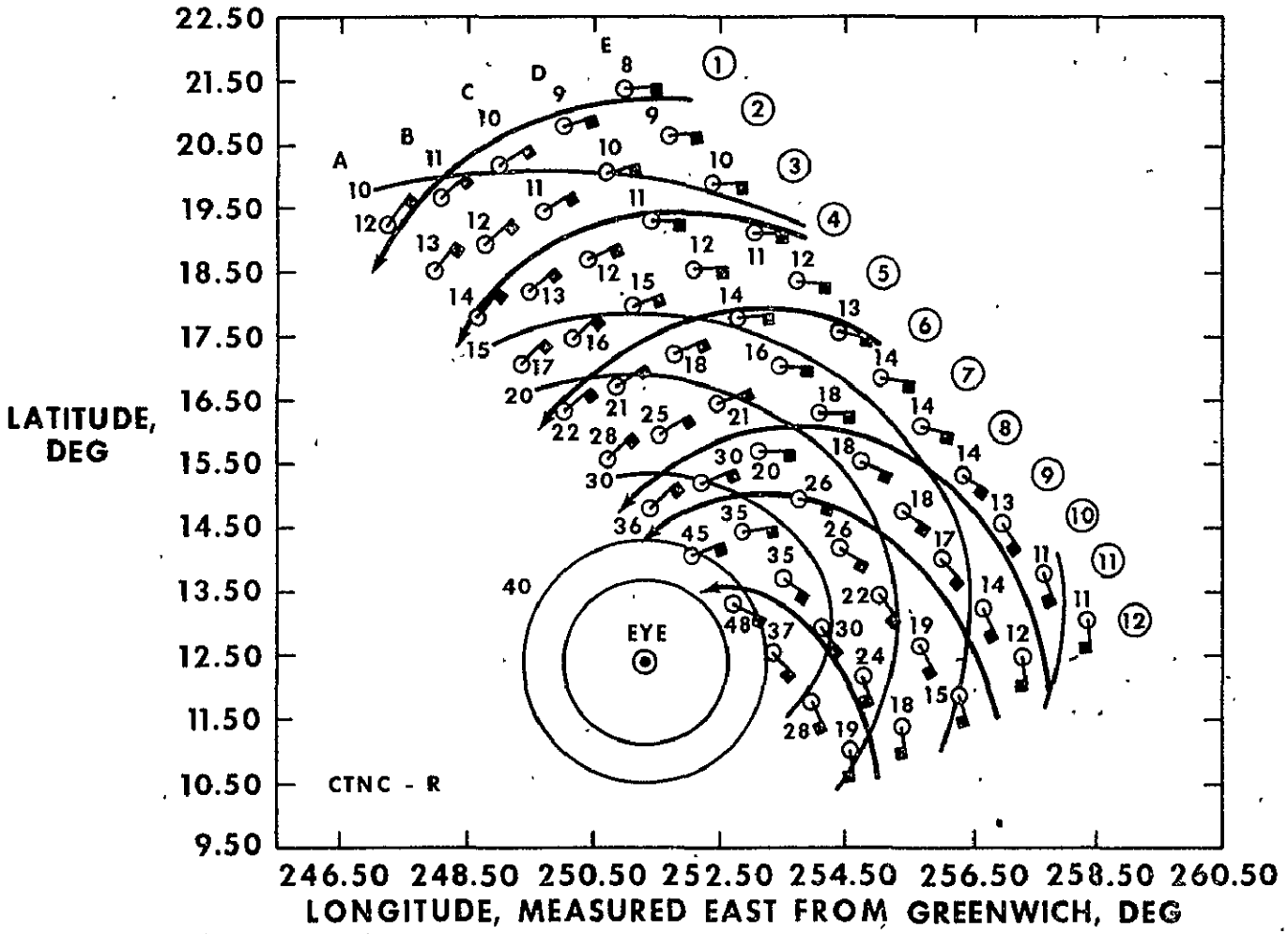

Figure 11. – Preliminary sketch of the Hurrican Ava wind field. (Univ. of Kansas)

relationship between σ_{OHH} and the windspeed a function of the form

$$\sigma_{OHH} = k_1 w_1^{k_2} \quad \ldots\ (1)$$

was used. This relationship has been observed for various NASA aircraft 13.3 GHz scatterometer missions. A least mean square computer fit yields a value of 1.89 for the constant k_2. The response of the radiometer to the hurricane is shown in figure 6. The radiometric antenna temperatures rise slowly up to about 30 knots surface wind and then rapidly up to 48 knots.

The dependence of the vertically polarized backscattering cross section (σ_{OVV}) on wind state for the June 5 and June 11 passes over Gulf of Mexico is shown in figure 12 [9]. These data have been corrected for the wind direction effects. The data suggests a simple prediction based on a computer fit. A functional dependence of the type given in equation (1) is suggested.

The analysis is continuing and the results to date indicate that a radiometer/scatterometer can be used to

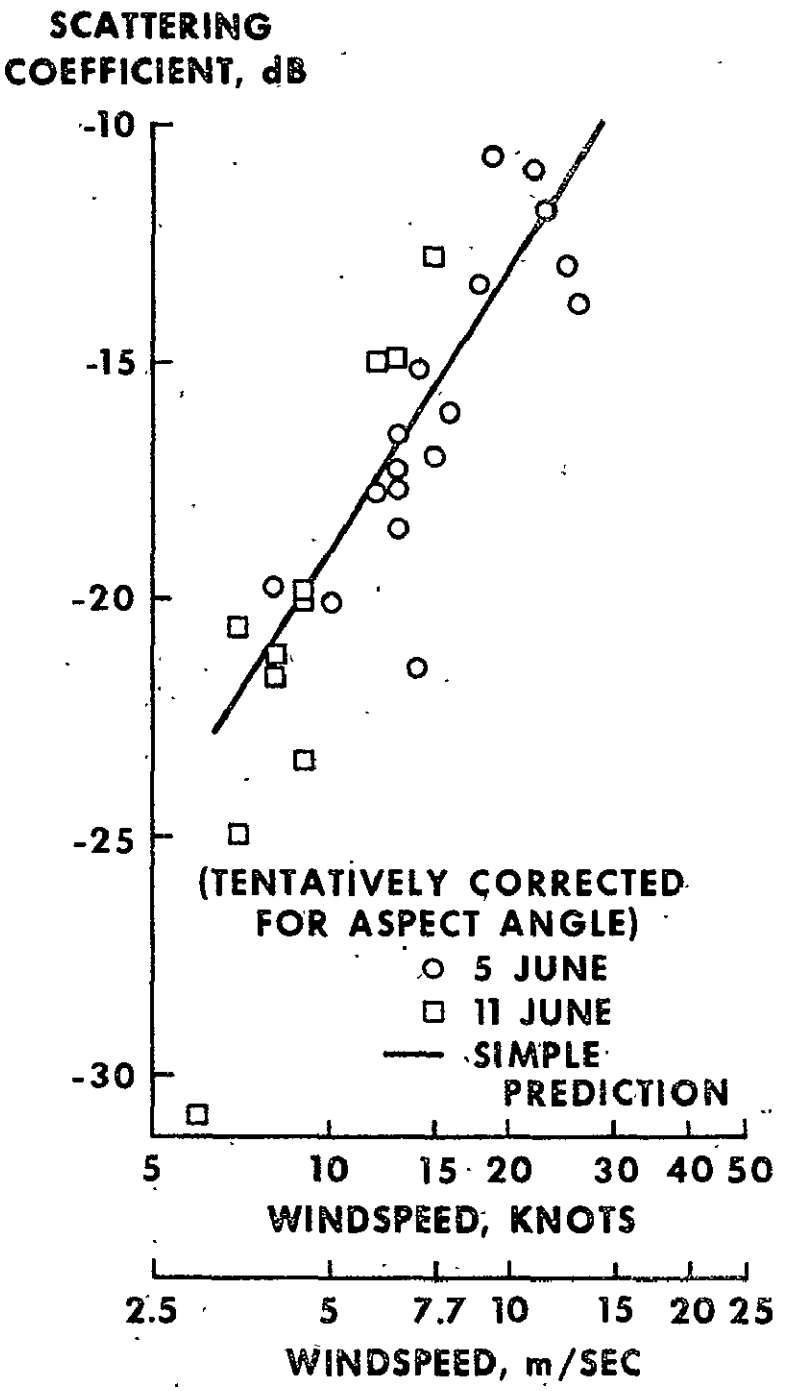

Figure 12. — Vertically polarized radar wind response at 50° incidence angle (Univ. of Kansas).

measure windspeeds up to 48 knots. Knowledge of waves and winds will permit locating more efficient ship routing, developing better weather forecasting models, planning better ship design to withstand wave impacts, designing better off-shore platforms, and most important, forecasting for coastal zones.

3.3.1.2 Measurement of soil moisture, type, and texture. Earlier studies using airborne and ground-based active and passive microwave sensors have demonstrated considerable promise in detecting soil moisture. Limited study of S-193 has confirmed the correlation between the response of active and passive microwave sensors and the soil moisture [15]. The results of this study for EREP pass on June 5, 1973, over Texas (GMT 18:00:37, CTC, R/S, pitch offset 29.4 degrees) will be briefly summarized here.

Figure 13 shows a composite precipitation map of the area (prepared from data for 5 days of rainfall/precipitation history before and including the time of pass). The rainfall history was computed using the following approximation to the soil moisture[15].

$$R_H = \sum_{i=1}^{5} K^{(6-i)} R_i \qquad \ldots\ (2)$$

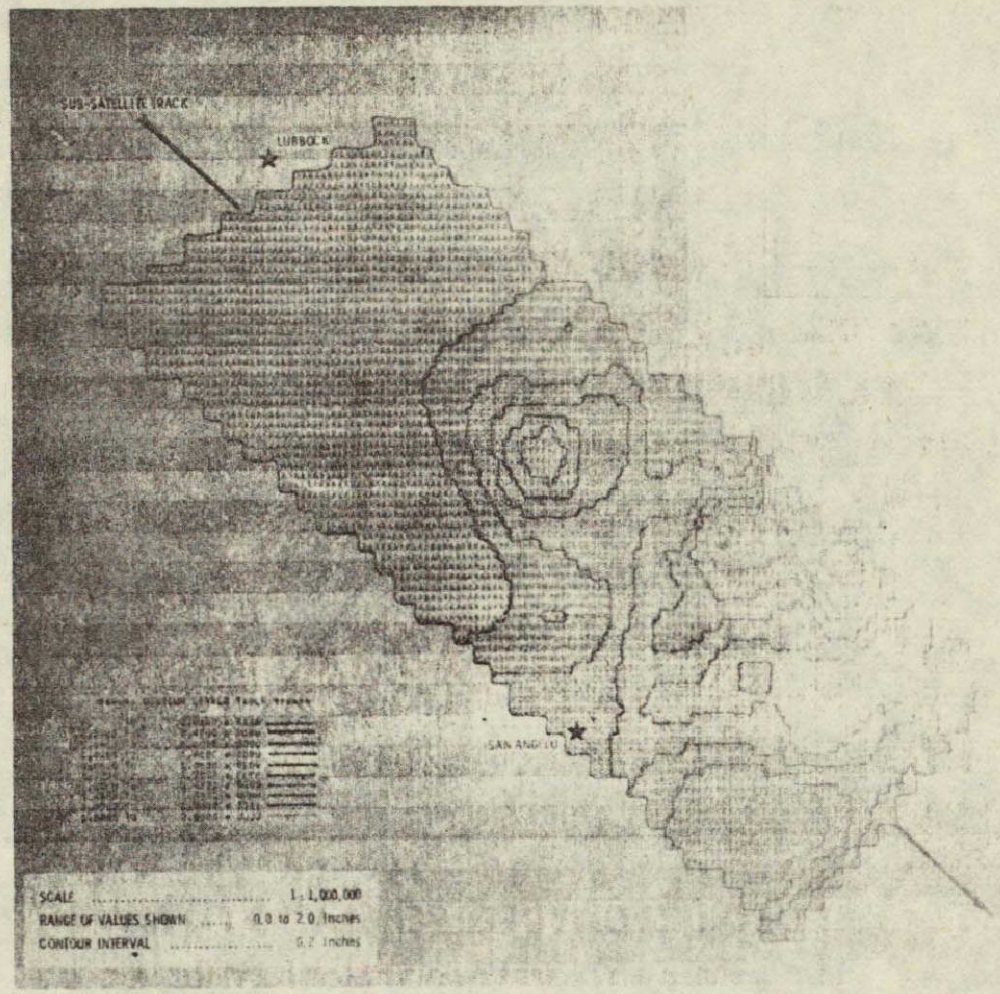

Figure 13. – Composite rainfall history - pass 5, day 156, 1800 G.m.t. (Univ. of Kansas)

In equation (2), K is a constant and R_i is the rainfall for the ith day. The data was obtained from 78 climatology stations within the reporting area. The data was interpolated to construct the map for entire pass. Rainfall up to 1.81 inches per day was reported. Figure 14 shows the S-193 radiometric temperature as a function of soil moisture for this pass. The dashed line is the regression line without the data point in the lower left. The correlation coefficient of -0.86 corresponds to the dashed line. For the entire set a correlation coefficient of -0.75 was obtained. When the effects of clouds and the ground's physical temperature are incorporated, emissivities can be computed using the following equation for the measured radiometric antenna temperature (T_a):

$$T_a = L(ET_g + T_{sc}) + T_u \quad \ldots\ (3)$$

In equation (3), L is the atmospheric transmittance, E is the scene emissivity, T_g is the ground temperature, T_{sc} is the upward scattered radiation, and T_u is the upward emission by the atmosphere. Figure 15 shows the emissivities calculated from the radiometric temperature interpolated data. The emissivity as a function of the soil moisture content determined from the radiometer data

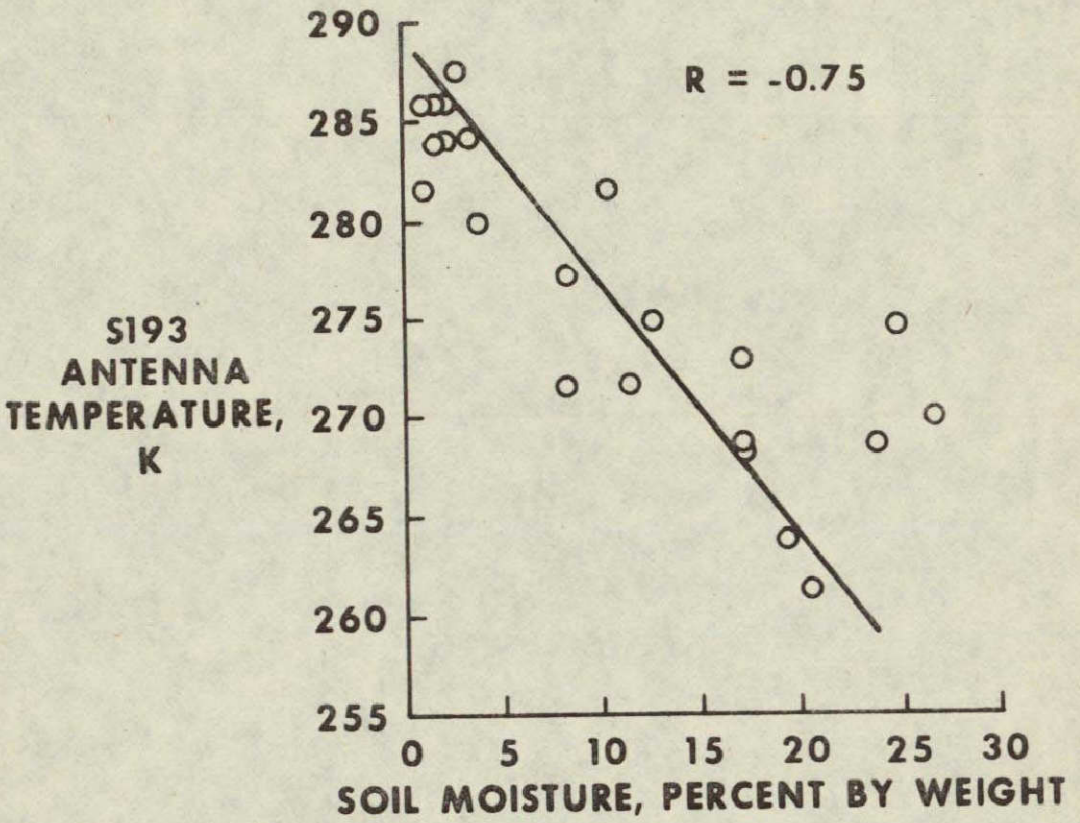

Figure 14. – The S193 radiometric temperature as a function of soil moisture for the June 5, 1973, EREP pass (Univ. of Kansas).

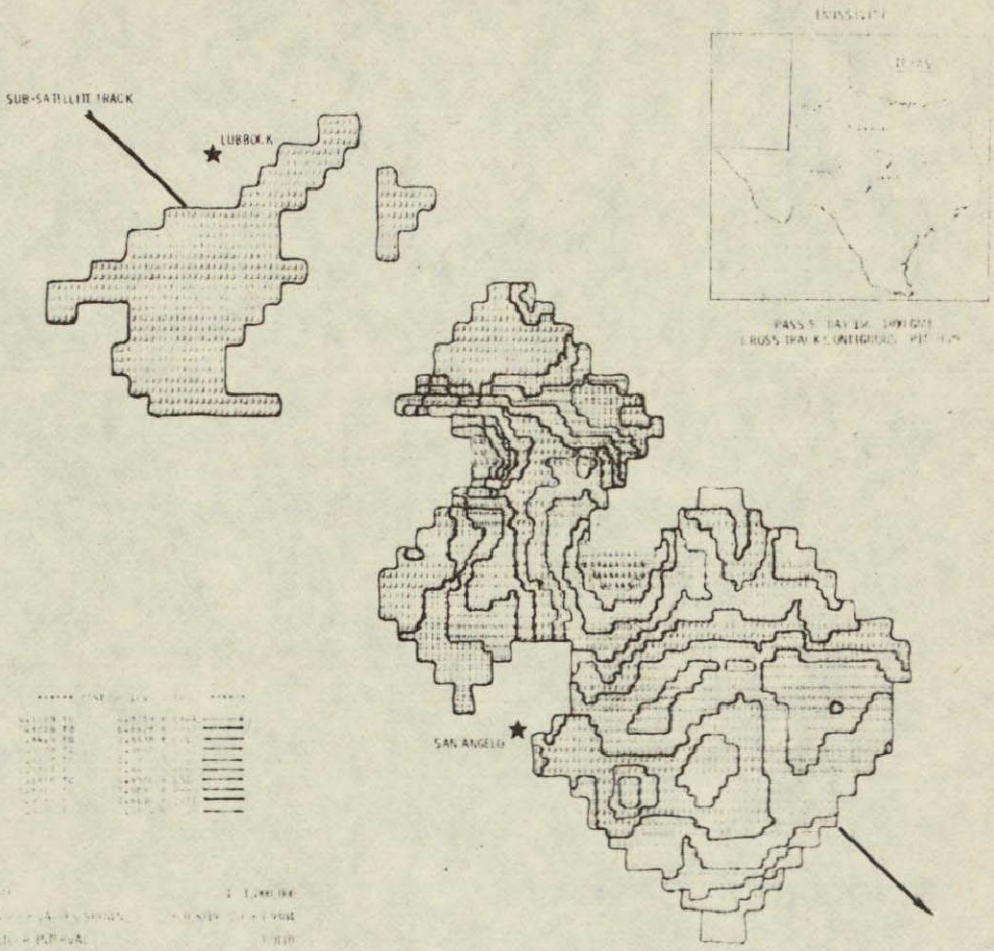

Figure 15. – Emissivity - pass 5, day 156, 1800 G.m.t. (Univ. of Kansas)

is given in figure 16. The correlation coefficient associated with a linear fit is -0.88, an improvement over the value computed directly from the radiometer data.

The scatterometer backscatter coefficient for the area under study is shown in figure 17.

The S-193 backscatter coefficient as a function of soil moisture is given in figure 18. For this data a correlation coefficient of 0.67 was obtained[15].

3.3.1.3 Identification of target types and surface parameters. S-193 scatterometer and radiometer data has been used to prepare false color photographs. Lakes, rivers, and areas of high rainfall rate have been identified independently of sunlight and cloud cover. The prediction of the root mean square slope was accomplished over the Great Salt Lake Desert area by using an appropriate scattering model and a computer fit to the data. Emissivities and power reflection constants were computed from radiometer and scatterometer data, respectively. From this the dielectric constants were also predicted[8]. Work is continuing on identifying crop types and conditions using S-193 data.

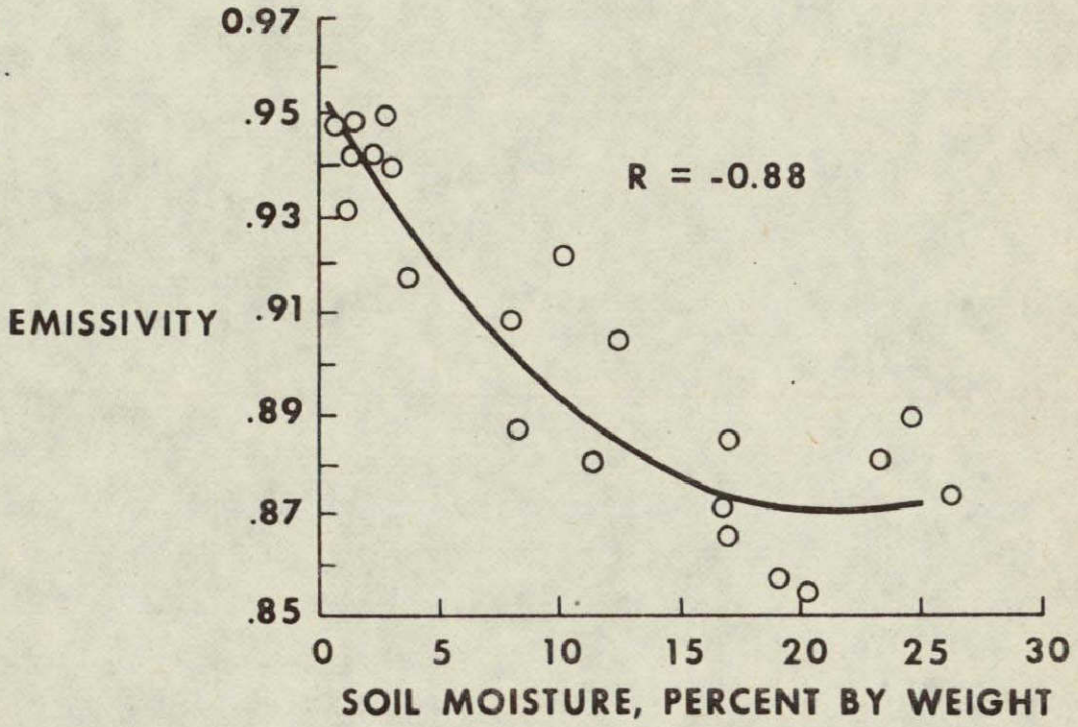

Figure 16. – Emissivity as a function of soil moisture content determined from Skylab S193 data (2.1-cm wavelength)(Univ. of Kansas).

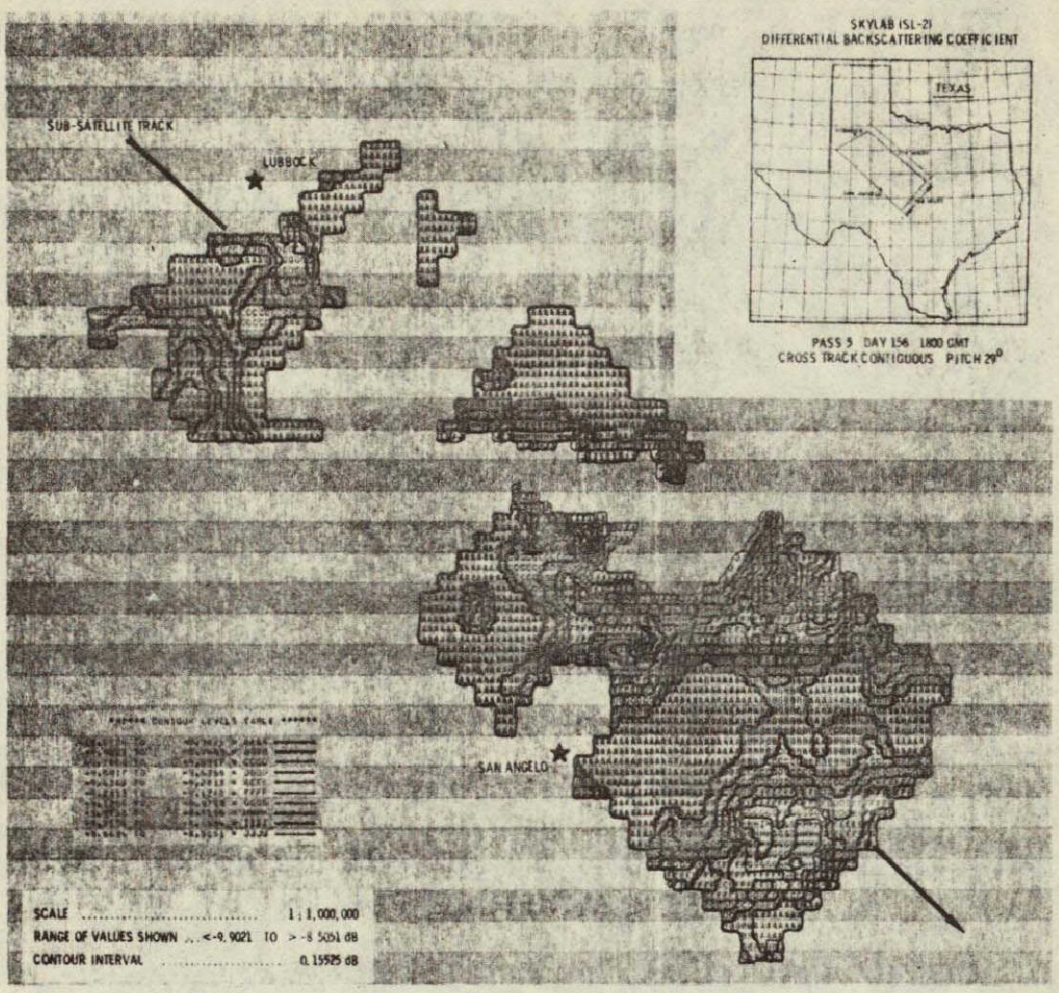

Figure 17. – Differential backscattering coefficient - pass 5, day 156, 1800 G.m.t. (Univ. of Kansas)

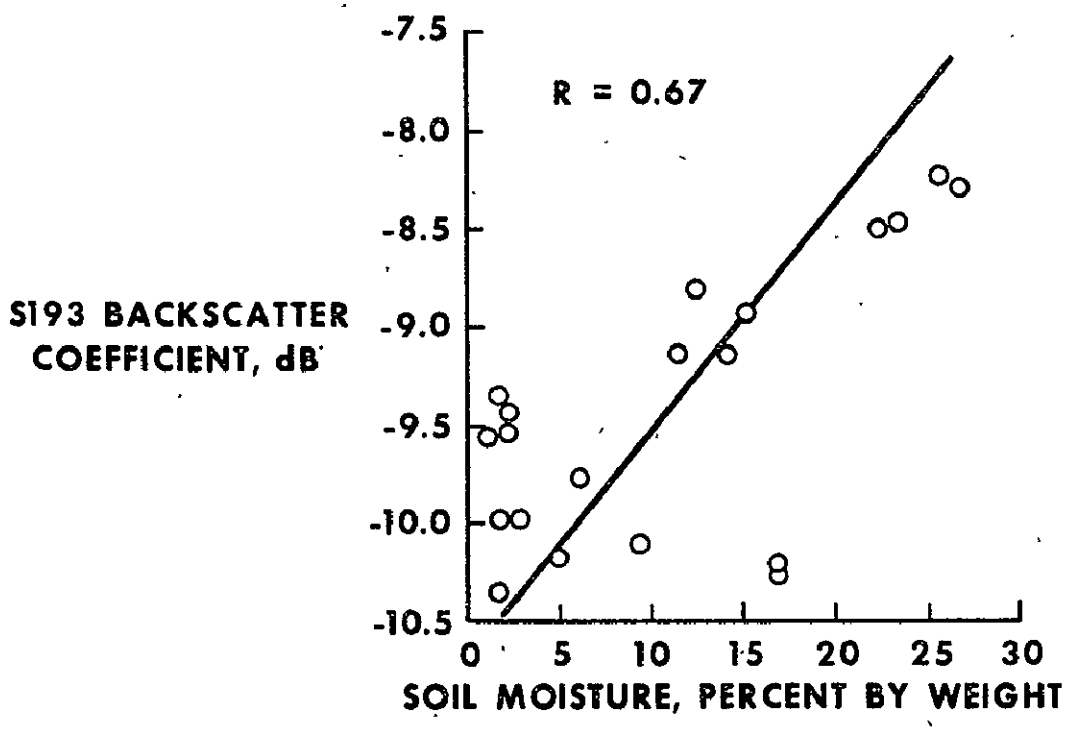

Figure 18. — The S193 backscattering coefficient as a function of soil moisture (Univ. of Kansas).

3.3.2 Altimeter

3.3.2.1 Shape of the geodetic profile and feasibility of measuring sea bottom topography. The information obtained from the S-193 altimeter experiment has considerably exceeded all expectations and has provided unique geodetic data. One of several examples of geodetic profiles obtained is presented in figure 19[16]. This example shows a comparison of the altimeter-geoidal data and the March-Vincent data developed from a 1 degree × 1 degree reference grid. In the S-193 altimeter, the range in meters is the difference between the altimeter-measured geoid and the reference ellipsoid as determined by the orbital data. It is denoted as "altimeter residuals." Both absolute and relative comparisons are shown. With the exception of the C-band radar tracking data (reported to have 5-meter root mean square uncertainty), the absolute displacements between S-193 and March-Vincent data may not be meaningful since these are largely indications of the long term errors in the orbital solutions. In figure 19 data from the pass over the vicinity of Wallops Island, Virginia, is given. The orbital data was obtained by a combination of the unified S-band tracking system and the NASA Wallops Space Center FPQ-6 radar. Figure 20 shows the location of the pass 9 ground track[16].

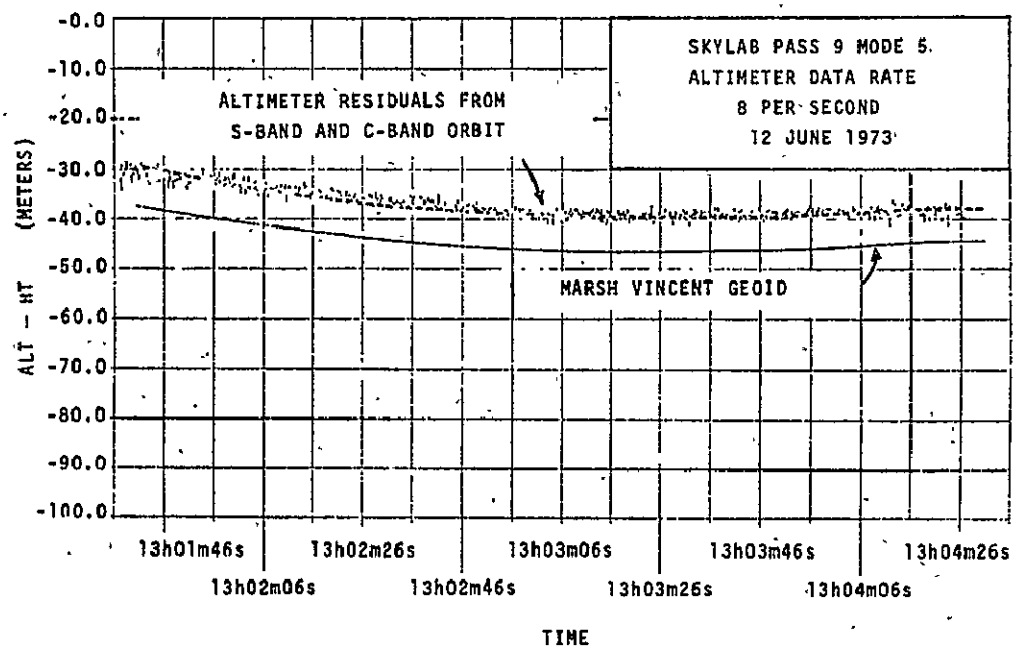

Figure 19. — Comparison of altimeter altitude residuals (from S-band and C-band determined orbit) with the Marsh-Vincent geoid in the vicinity of Wallops Island, Virginia (NASA/WI).

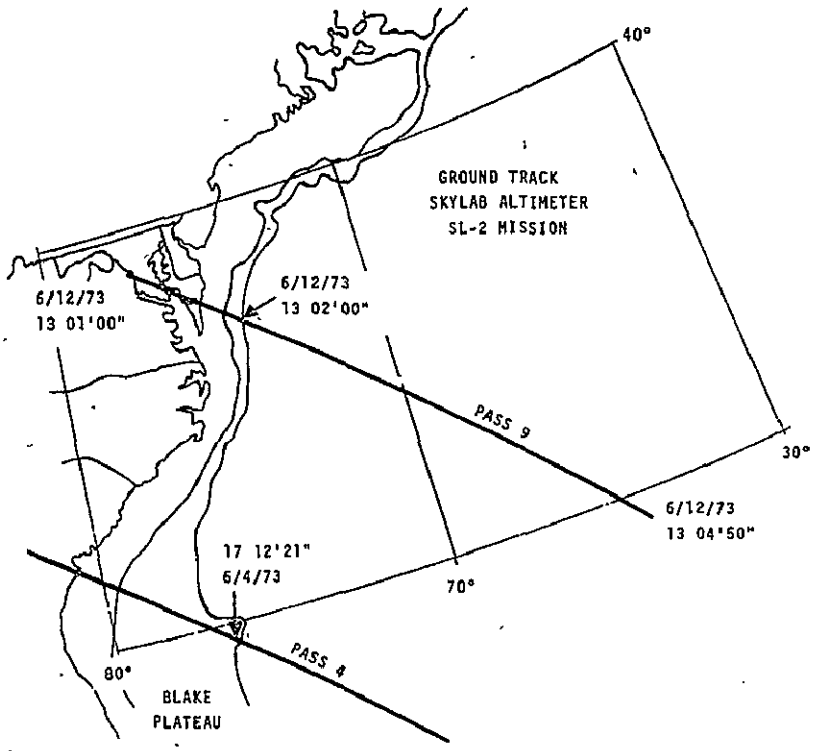

Figure 20. — Ground tracks for passes 4 and 9 of Skylab Mission SL-2 (NASA/WI).

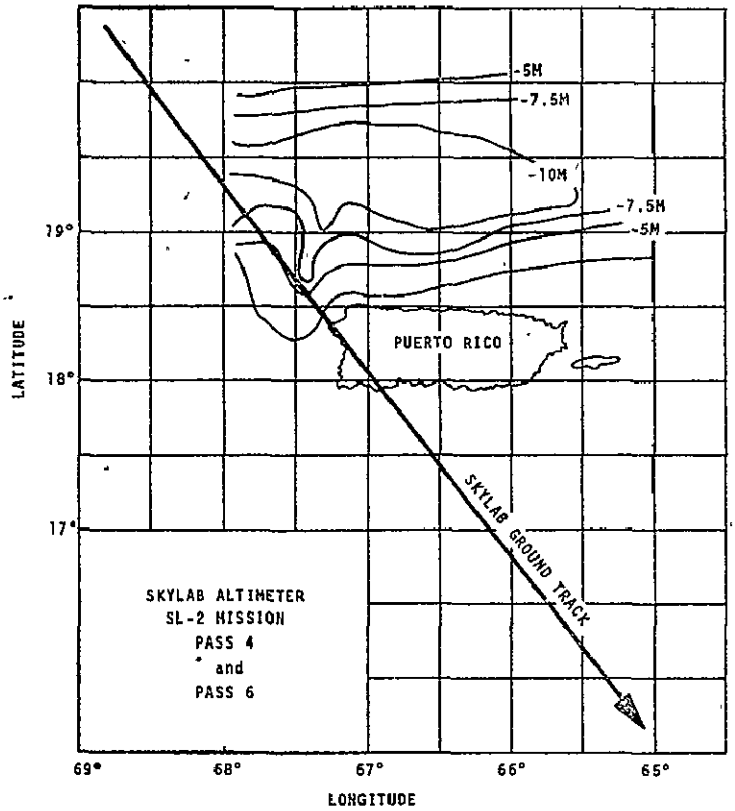

Figure 21. — Ground track for the Puerto Rican Trench area data shown in figures 11 through 14 (NASA/WI).

Skylab EREP passes 4 and 6 were flown over a known geodetic anomaly — the Puerto Rican Trench (figure 21). These passes have essentially the same ground track. The trench gravitational anomaly is manifested in a mean sea level depression of about 10 meters in the first 20 seconds of data. The large increase in residuals given in figure 22 near 40 seconds from the left side of the record is due to island land scatter. The S-193 data shows adequate overall agreement with the Puerto Rican Trench region data given by Vincent and the ever closer relative agreement with data from Von Arx[16].

Geodetic surface variations with an accuracy of 5 meters to 20 meters on a global scale have been measured using S-193 altimeter data[16].

Figure 23 shows the altimeter residuals in the beginning in the vicinity of Charleston, South Carolina, for EREP pass 4. The ground track for figure 23 is given in figure 20. Figure 23 also shows a record of the ocean bottom profile. It is intriguing to note the correlation between the altimeter data and the bottom features. It should be noted that at the "Change of Pointing Angle," there was a programmed

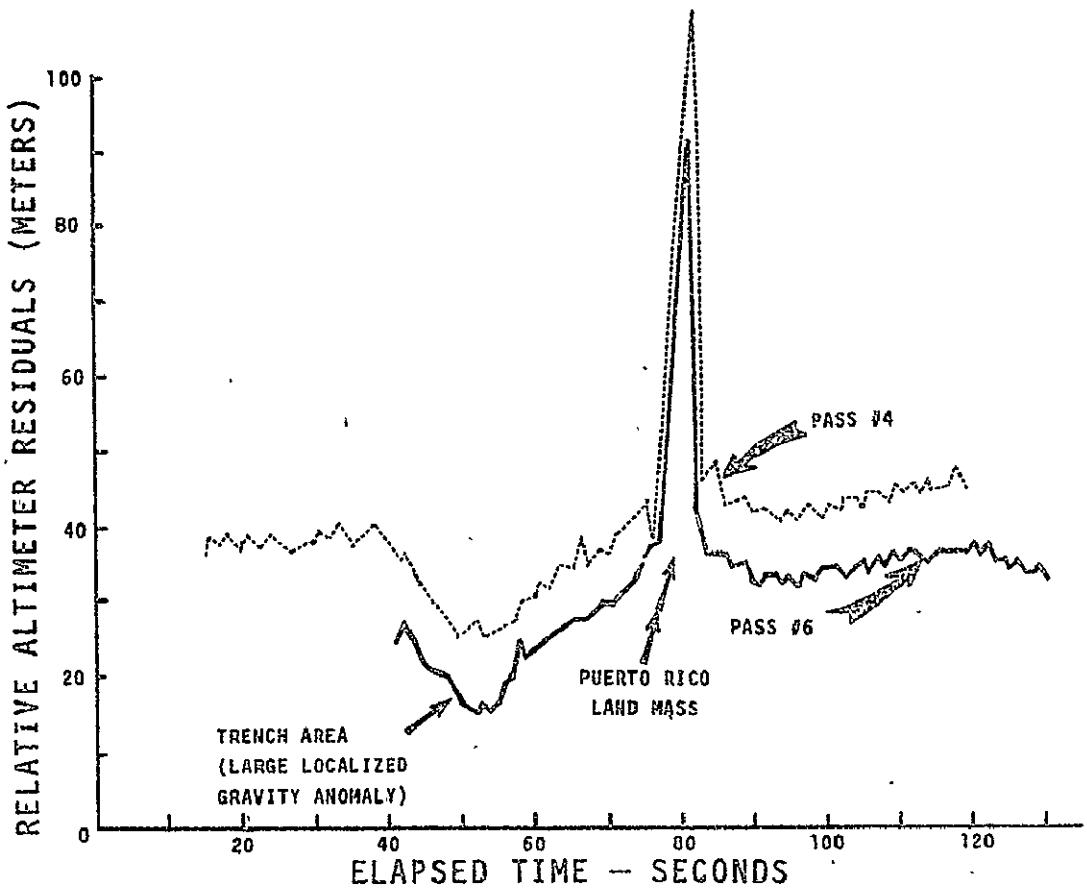

Figure 22. — Comparison of Puerto Rican Trench area data from passes 4 and 6, Skylab Mission SL-2, on corrected time scale (NASA/WI).

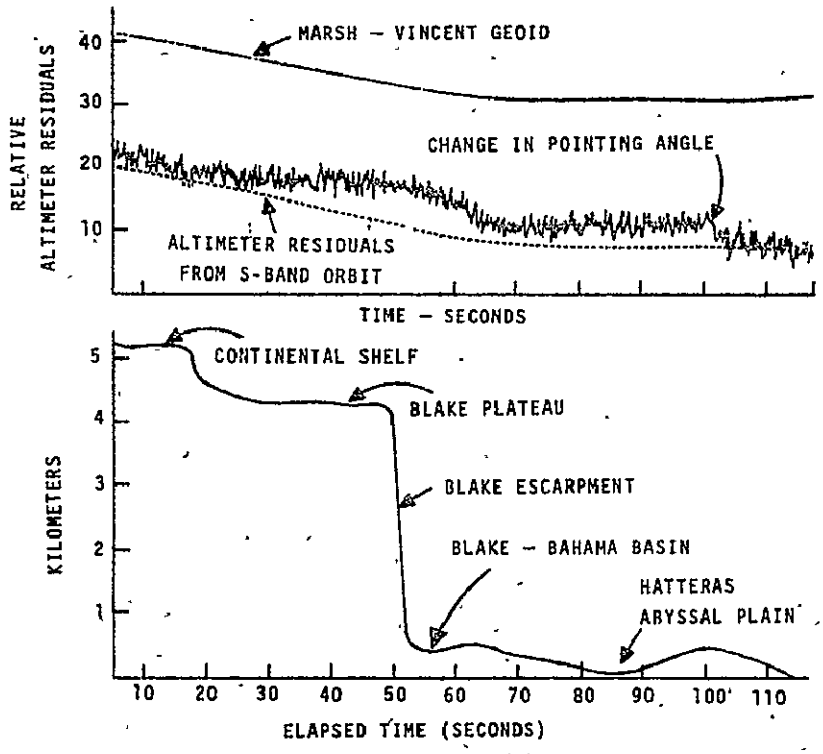

Figure 23. – Comparison of altimeter altitude residuals (from S-band determined orbit) with the Marsh-Vincent geoid and the corresponding undersea topography (in the vicinity of the Blake Escarpment) (NASA/WI).

altimeter submode change altering the antenna pointing angle by about 0.5 degrees. The altimeter record discontinuity at this point is the result of an attitude and not an altitude change. A few other examples of this correlation for S-193 altimeter data have been noted[16].

3.3.2.2 Pointing angle determination. The S-193 nadir align mode gave pointing accuracy to within ±0.5 degrees[16] A better estimate for determining antenna pointing angle was developed using the experimentally obtained pulse shapes. These pulse shapes were compared with these calculations using altimeter antenna beamwidth, 100-ns pulse width, averaging time, and altitude. Using this procedure, antenna pointing angle can be resolved to within ±0.05 degrees. For off-nadir angles it can be resolved in the range of 0.25 to 0.8 degrees. Figure 24 shows the results of this comparison. The 0.05 degrees accuracy figure has been empirically determined to be the accuracy obtainable[16].

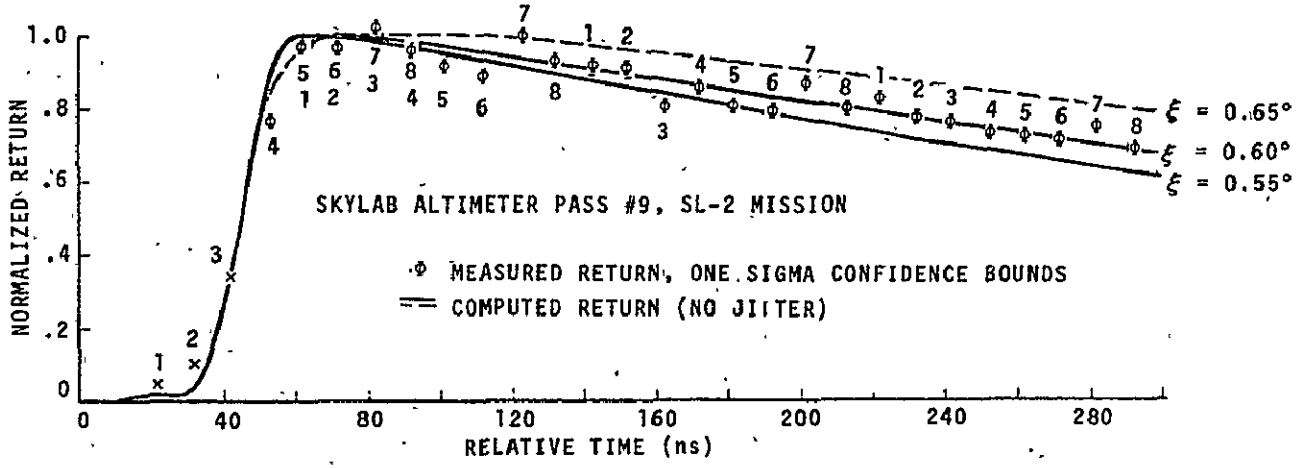

Figure 24. – Comparison of measured and theoretical (neglecting tracking loop jitter) mean return waveforms for a 10-ns transmitted pulse width (pass 9, mode V, DAS-3)(NASA/WI).

3.4 DATA ACQUISITION AND MISSION REQUIREMENTS FOR FUTURE SPACECRAFT MICROWAVE SENSORS

The experience gained from the S-193 program has resulted in several procedures for mission planning. Regions of particular interest to the study of certain phenomena must be identified before the data acquisition pass. Computer programs have been developed showing times and conditions for possible data acquisition based on sensor and mission constraints. These computer-generated sequences of mission events take into account the mandatory and desirable conditions, such as cloud cover, sunlight, and other parameters. These programs will be useful for future spacecraft microwave sensors.

4.0 CONCLUSION

The National Aeronautics and Space Administration has advanced the concept of Earth observations using airborne and spaceborne remote sensors for nearly a decade. Considerable attention has been given to the optical and infrared scanner systems. Microwave sensors have also been used, although to a far lesser extent.

The night, day, and nearly all weather capabilities of microwave sensors have received new emphasis recently, since NASA is interested in obtaining remote sensor data with the highest efficiency.

S-193 should be considered as a first step toward expanding microwave technology for remote sensing of Earth phenomena. Scatterometers and radiometers can provide capability for measuring ocean surface winds up to 45 knots. Sea state information can also be gathered from vertical backscatter and antenna temperature. Future systems call for considerable improvement on precision, resolution, and signal-to-noise performance.

Recently, considerable progress has been in the manufacture of microwave semiconductor components and microwave-integrated circuits. This should mean improvement in the

reliability of microwave sensors. The rapid development of minicomputers and microcomputers makes onboard processing attractive for low and medium data acquisition rate systems. Future sensor development must include feasibility studies for onboard data processing.

One area which needs improvement is how the radiometer and scatterometer data should be displayed for oceanographers or other users. False color photos, computer contour maps, or other types of displayes should be explored to convey information to the users not familiar with the intricacies of microwave sensors.

Altimeters indicate an increasingly accurate detection of dynamic ocean features, such as waves, tides, and currents; mapping of geoid; and positioning and density determination of underwater topography. The S-193 altimeter has provided valuable data for the design and development of future satellite altimeter. The GEOSC altimeter serves as one example.

The decade ahead calls for side-looking imaging radars for ocean and land remote sensing. Toward achieving an optimum design for such an imaging radar, the S-193 acquired data will prove extremely valuable. The microwave system will have to perform for extended periods in space. Serious

consideration should therefore be given to making future sensors repairable in space. This would allow highly useful sensors to be scheduled as part of the Space Shuttle program.

ACKNOWLEDGE

The author wishes to acknowledge the contributions made by D. J. Pounds, Lockheed Electronics Corp., and Dr. R. K. Moore, University of Kansas, to this report.

5.0 REFERENCES

1. Historical Logbook, S-193 Microwave Radiometer/ Scatterometer/Altimeter. General Electric Corporation, Document No. 72 SD4234, Rev. A, Vols. 1 through 10, October 1972.

2. NASA Johnson Space Center: "Earth Resources Production Processing Requirements for EREP Electronic Sensors", PHO-TR-524 revision A, May 10, 1973, with change 1.

3. NASA Johnson Space Center: "Earth Resources Experiment Package Sensor Performance Report, Vol. IV (S193 Rad/ Scat)," MSC-05528.

4. Krishen, K., and D. J. Pounds, "S-193 Radiometer and Scatterometer Sensor Mathematical Models", Lockheed Electronics Company, Inc., Technical Report LEC-1741, Houston, February 1974.

5. NASA Johnson Space Center: "Earth Resources Experiment Package Sensor Performance Report, Vol. V (S193 Alt.), MSC-05528.

6. Krishen, K., "Quick-Look Evaluation of Hurricane Ava S193 Scatterometer Data", Lockheed Electronics Company Memorandum 642-788, August 1973.

7. Potter, A. E. et. al., "Summary of Flight Performance of the Skylab Earth Resources Experiment Package (EREP)", Proceedings of the Ninth Conference on Remote Sensing of Environment", Ann Arbor, Michigan, April 1974.

8. Krishen, K., Remote Sensing of Surface Parameters Using Skylab S193 Radiometer/Scatterometer Data", Lockheed Electronics Company Memorandum, LEC-3980, July 1974.

9. Moore, R. K., J. P. Claassen, A. C. Cook, D. L. Fayman, J. C. Holtzman, A. Sobti, W. E. Spencer, F. T. Ulaby and J. D. Young, W. J. Pierson, V. J. Cardone, J. Hayes and W. Spring, R. J. Kern, N. M. Hatcher; Simulataneous Active and Passive Microwave Response of the Earth — The Skylab Radscat Experiment, presented at the 9th International Symposium on Remote Sensing of Environment, Ann Arbor, Michigan, April 15, 1974.

10. Pierson, W. J., The Scientific Justification of a Radar Scatterometer and a Passive Microwave System on Seascat A, Submitted to the Seascat A User Agency Committee and NASA Active Microwave Workshop, July 1974.

11. Krishen, K., Contribution to Ocean Panel Including Reports on Some Sea Return Experiments, Ocean Surface Windspeed Sensing and Scatterometers, Tech. Report LEC-3896, Lockheed Electronics Company, Inc., July 1974.

12. Cardone, V., W. Pearson, R. Moore and J. Young, "Preliminary Report on Skylab S193 Radscat Measurements of Hurricane Ava", City University of New York, University Institute of Oceanography Report, No. 23, October 1973.

13. Ross, D., et. al., "A Remote Sensing Study of Pacific Hurricane Ava", Proceedings of the Ninth Conference on Remote Sensing of Environment", Ann Arbor, Michigan, April 1974.

14. Hayes, J., et. al.: A Preliminary Analysis of the Surface Truth Data to be Correlated with the Skylab II Data Obtained for the S193 Microwave Investigators. City University of New York, Informal Report, August 1973.

15. Eagleman, J. R. and F. T. Ulaby, "Remote Sensing of Soil Moisture by Skylab Radiometer and Scatterometer Sensors" communicated to PIMO/NASA.

16. McGoogan, J., Miller, L., Brown, G. and Hayne, G., "The S193 Radar Altimeter Experiment", Proceedings of the IEEE, Special Issue on Radar Technology and Applications, June 1974.